Environmental Earth Sciences (2018) 77:674
https://doi.org/10.1007/s12665-018-7857-9

AUTHOR COPY

ORIGINAL ARTICLE

Hydro-geochemical characteristics of the groundwater resources in the southern part of the Red River's Delta plain, Vietnam

Hoan V. Hoang[1] · Lam V. Nguyen[1] · Nhan D. Dang[2] · Frank Wagner[3] · Nhan Q. Pham[4]

Received: 2 January 2018 / Accepted: 18 September 2018
© Springer-Verlag GmbH Germany, part of Springer Nature 2018

Abstract

In this study, the origin and recharge areas as well as the chemistry of the groundwater in the southern part of the Red River Delta plain, in Thai Binh, Nam Dinh and Ninh Binh provinces (North Vietnam) was investigated by using isotopic techniques combined with geochemical analysis. Groundwaters under the study were those that are available in the Holocene, Pleistocene, Neogene and Triassic aquifers. Groundwater in the Holocene aquifer is brackish of Na–Cl type with an electric conductivity as high as up to 6000 µS cm^{-1}. The water in the shallow aquifer comprises three end-members: the local precipitation, Red River's water and intruded seawater. Groundwater in the Pleistocene, Neogene and Triassic aquifers in the Southwest of the study region is fresh containing less than 1 g L^{-1} of total dissolved solids and is characterized by the Ca–Na–HCO_3 type. However, groundwater in the deep aquifers in the Northeast area is brackish of Na–Ca–Cl–HCO_3 ion type containing more than 1 g L^{-1} TDS. The chemistry of groundwater in the study region is controlled by three processes, namely the incongruent dissolution of the biogenic high Mg-calcite, the reduction of sulphate and iron oxyhydroxide with organic matters present in the aquifers. The salinity in deep aquifers in the NE was attributed to the diffusion of saline pore water from aquifer or/and aquitard deposits to the recharge water. Groundwater in the Pleistocene, Neogene and Triassic aquifers in the study region seem to have meteoric origin with long traveling time and it mixed with the saline pore water that migrated from the aquifers sediments, as it was evident from the water isotopic compositions. The isotopic compositions of water (δ^2H and $\delta^{18}O$) in the Neogene and Triassic aquifers are similar to that found in the Pleistocene aquifer suggesting the aquifers are hydraulically connected to each other due to the over-extraction rate of fresh water from the latter aquifer. Recharge area of groundwater in the Pleistocene and Neogene aquifers is suggested to be from the NW extension of the region and out crops at a highland at an altitude of 140–160-m above sea level (masl). The recharge water flows from northwesterly towards southeasterly to the sea coast. The results of the ^{14}C-dating for groundwater combined with the hydraulic heads distribution in the deep aquifers revealed that the saline groundwater is flowing from the NE and backwards from the sea side to the production well field in the center of the region due to the high rate of groundwater mining. In order to mitigate the saltwater intrusion and avoid deterioration of the quality of the groundwater that is currently being mined and supplied to the local population, it needs to develop and implement an appropriate strategy for the groundwater resource management in the region.

Keywords Saltwater intrusion · Isotopic composition · ^{14}C-dating · Red River's Delta · Vietnam

Electronic supplementary material The online version of this article (https://doi.org/10.1007/s12665-018-7857-9) contains supplementary material, which is available to authorized users.

✉ Hoan V. Hoang
hoanghoandctv@gmail.com

[1] Hanoi University of Mining and Geology, Duc Thang Ward, North Tu Liem District, Hanoi, Vietnam

[2] Vietnam Association of Hydrogeology, Nghia Do Ward, Cau Giay District, Hanoi, Vietnam

[3] Federal Institute for Geosciences and Natural Resources (BGR), Stilleweg 2, 30655 Hannover, Germany

[4] Hanoi University of Natural Resources and Environment, Phu Dien, North Tu Liem District, Hanoi, Vietnam

Published online: 25 September 2018

Introduction

The Red River Delta plain (RRDP), covering an area of approximately 15,000 km^2 is situated across the northern part of Vietnam and is one of the two most productive deltas in the country. The abundant water resource from the river and soil enriched with nutrients has facilitated agricultural activities of the region. Deltaic population density of 1300 heads km^{-2} creates a heavy pressure on natural resources' consumption, particularly that of fresh groundwater. A recent survey (ADB 2016) report on availability of 50–60 L of freshwater per person per day signifies the vulnerability where the Vietnamese Government target is close to 90–100 L day^{-1} per capita. In RRDP, water is used for irrigation, industrial and domestic purposes out of which irrigation consumes around 95% of the 83.031 km^3 annual production (Frenken 2012). In the RRDP, groundwater is the main source of domestic usage water. Reports state that the groundwater storage capacity of the RRDP is over 23 billion m^3, out of which roughly 20% is located in the southern part, i.e., Thai Binh, Nam Dinh and a part of the Ninh Binh provinces (Le et al. 2000; Bui et al. 2011). The sources for the recharge are precipitation and the Red River system (Bui et al. 2011).

Industrial groundwater exploitation in the southern part of the RRDP has reached 300,000 m^3 a day from the initial operational usage in 1982 of 94,949 m^3 a day (Doan 2015; Hoang 2014). This over exploitation has led to a drawdown rate of 0.6–0.7 m a year since 1995 (Wagner et al. 2011).

The quality of groundwater in the RRDP has been intensively studied since 2000. It has been revealed that the water in aquifer at a depth up to 30 m from the surface is contaminated with salt or iron, manganese, arsenic and ammonium and is not suitable for domestic usage purposes (Berg et al. 2001; Le and Doan 2005; Postma et al. 2007; Larsen et al. 2008; Norrman et al. 2008, 2015; Pham 2004; Luu et al. 2012). The fresh water extracted for daily use in the region is mainly from depths below 70–80 m from the ground surface (deep aquifers).

The origin and chemistry of groundwater in the entire RRDP were studied by a number of researchers, e.g., Luu et al. (2012) and Nguyen et al. (2014, 2015). The groundwater in the RRDP was classified into three types: fresh, low saline and high saline (Luu et al. 2012; Nguyen et al. 2015). Vietnamese hydrogeologists have drawn conclusions that fresh groundwater recharges across mountainous areas in the NW and discharges in the SE into the sea. This hypothesis is based on the topography of the Delta without any conclusive evidence (Bui et al. 2011). From the geochemical data of groundwater Nguyen et al. (2014, 2015) concluded that weathering of rock-forming minerals in the upstream areas and seawater intrusion along the coast tract have a significant say on subsurface water hydrogeochemistry. However, in these reports the role of organic matters (OM) present in the aquifer deposits of the Delta was not considered (Nguyen et al. 2014, 2015). Organic matter in the aquifer sediments seems to play an important role in the mobilization of pollutants like heavy metals or nitrogen through the redox reactions. For example, one of the reasons behind arsenic (As) pollution in groundwater across deltaic plains was attributed to the reduction of iron-oxyhydroxide adsorbed As by OM (McArthur et al. 2004; Zheng et al. 2004; Postma et al. 2007). However, the evolution of groundwater and controlling geochemical processes are not comprehensively conclusive.

The present study intends to investigate in detail the recharging area, geochemical characteristics and controlling processes thereof across southern RRDP. These findings hold significant potential for the strategic development and sustainable exploitation of fresh aquifers that seem to be confines to the deep aquifers of the region.

Study site

The study site encompasses the southern RRDP that comprises a part of Thai Binh, Nam Dinh and Ninh Binh provinces (Fig. 1a). The national monitoring network for groundwater resources has been well established in the region since 1990 and it was supplemented by the boreholes recently installed under the Project entitled "Improving Groundwater Protection in Viet Nam (IGPVN)" (Wagner et al. 2011; Lindenmaier et al. 2011) supported by the German Government. The study site (Fig. 1a) occupies an area of 4600 km^2 where 4.848 million habitants are residing (NDPSO 2014).

The climate in the study region is sub-tropical with a rainy season from May to October and a dry season from November to April. During the rainy season, precipitation ranges from 1400 to 1750 mm and from 150 to 300 mm during the dry season. The potential annual evaporation in the region is in the range of 700–800 mm (Nguyen and Nguyen 2004). The monthly average temperature varies between 16 °C and 35 °C with the lowest temperature in January and the highest in July (Nguyen and Nguyen 2004).

Hydrology of the study site

The river network of the study region is very dense. Almost 3% of the land area is covered by rivers and irrigation canals (Kasbohm et al. 2013). The main rivers flowing through region are Red River and Day River (Fig. 1a). Dao and Ninh Co Rivers (Fig. 1a) are tributaries of Red River that have been man-made during the Tran's Dynasty in the thirteenth century to control floods during the rainy season

and for irrigation purposes in the dry season. Red River annually discharges 119,837 km^3 of water into the Ton Kin Gulf, Eastern Sea (former it was the South China Sea), and discharge from Day River is 1848 km^3 annually (Luu et al. 2010).

The tidal regime in the region is diurnal with a level ranging from 2.6 to 3.6 m as recorded at Quang Phuc hydrological monitoring station, around 50 km NE of the mouth of Red River (NCMH 2012).

Geology and hydrogeology of the study region

The geology and hydrogeology of the study region drawn for a NW-SE oriented cross-section AB is shown in Fig. 1b. The sequence of geological strata discovered along the cross-section AB is identical with those found for a cross-section extending from the NW apex of the Delta (in Ha Noi city) towards the sea shore in Thai Binh province (Bui et al. 2011). The only difference between the results of geological formation found in our study and those reported in the Bui et al. (2011) was the thickness of each geological stratum.

The Red River Delta plain sediments consist of Holocene, Pleistocene and Neogene deposits (Bui et al. 2011). Holocene deposits in study region are found from elevation of + 2 m to − 15 m (layer #1, Fig. 1b) and contain alluvial sediments and fine sand with disseminated wood debris as well as biogenic calcite such as shells and carbonate mud, etc. (Tanabe et al. 2003). The Holocene sediment layer forms the Holocene unconfined aquifer (Holocene) where water exists within sediment pores (Le et al. 2000; Bui et al. 2011). Below Holocene deposit there is a silty-clay layer of Holocene and Pleistocene with a thickness up to 100 m (layers #2 and #3, Fig. 1b) that forms an aquitard, a low permeable clay layer, to separate Holocene aquifer from deeper aquifers. Following aquitard, in the NE area there are medium to coarse fluvial and marine sediment deposits, but in the SW area there are silty and fine to medium grained marine sand deposits of Pleistocene with a thickness up to 75 m (layer #4, Fig. 1b). The NE and SW areas were presumably separated from each other by boundary between blue and light brown color areas in the Nam Dinh province (Fig. 1a). The NE area comprises the northern part of Nam Dinh and Thai Binh provinces. The SW area comprises the southern part of Nam Dinh province and a part of Ninh Binh province (Fig. 1a). The sediment in Pleistocene deposit contains disseminated fragments of organic materials like wood remnants as well as biogenic carbonate such as shells, skeletal debris, etc. (Tanabe et al. 2003). The porous water in Pleistocene sediment layer forms Pleistocene confined aquifer (Le et al. 2000; Bui et al. 2011). The underlying Neogene silt and sandstone deposits are located from 120 to 130 m to 220–230 m below the surface (layer #5, Fig. 1b). The water existing in the consolidated Neogene formation forms the Neogene water bearing layer or Neogene aquifer. The Mesozoic stone basement is located from 230 m below the ground surface (layer #7, Fig. 1b). The block #6 is Mesozoic limestone found in the West of the RRDP. The water in fractured Mesozoic rocks basement constitutes Triassic water zone (Fig. 1b).

Methods

In this study isotope techniques combined with chemical analyses of the ionic contents of local precipitation, water from the Red River and groundwater samples, are applied. Results of chemical analyses give an insight into geochemical processes controlling quality, while isotope techniques provide evidences to verify the mechanisms behind geochemical processes. The isotope techniques used in this study include: (1) tritium (^{3}H) and carbon-14 (^{14}C) dating to verify recharge areas, the patterns of groundwater flows and to estimate the flow rate of recharge water; (2) determination of water stable deuterium (^{2}H) and oxygen-18 (^{18}O) isotopes composition to delineate the hydraulic interaction between local precipitation and groundwater and the inter-connection between aquifers as well as to examine the recharge area; (3) determination of the carbon-13 (^{13}C) composition in the dissolved inorganic carbon (DIC) to evaluate the type of mineralization of groundwater existing during water seepage and recharge conditions. All these approaches were successfully applied in hydrogeological studies worldwide, e.g., Zhu (2000), Kalin (2000), Mook (2001), Erickson (1983), Clark and Fritz (1997), Glynn and Plummer (2005) and Sánchez-Murillo et al. (2015). As carbon is not a constituent of water molecule, to derive the age of groundwater with an acceptable uncertainty from measured ^{14}C-activity in the DIC, initial correction of ^{14}C-activity was carried out before its passage to saturated zone. The geochemical processes which potentially modify amount of ^{14}C in DIC during water seepage through unsaturated zone and model applied for correction is presented in detail in "Groundwater residence time (the ^{14}C-age) estimation".

During the water cycle, composition of water stable isotopes (^{2}H and ^{18}O) will be changed due to the isotopic fractionation effect. During evaporation, heavy isotopes tend to be enriched in the liquid remaining fraction and when condensation occurs they tend to be enriched in the condensate. The extent of the deuterium and oxygen-18 fractionation during phase transformation was expressed in delta notation as follows:

$$\delta^2\mathrm{H} = \left(\frac{R_{2_{\mathrm{H,sample}}}}{R_{2_{\mathrm{H,std}}}} - 1\right) \times 1000, \quad (1)$$

$$\delta^{18}\mathrm{O} = \left(\frac{R_{18_{\mathrm{O,sample}}}}{R_{18_{\mathrm{O,std}}}} - 1\right) \times 1000, \quad (2)$$

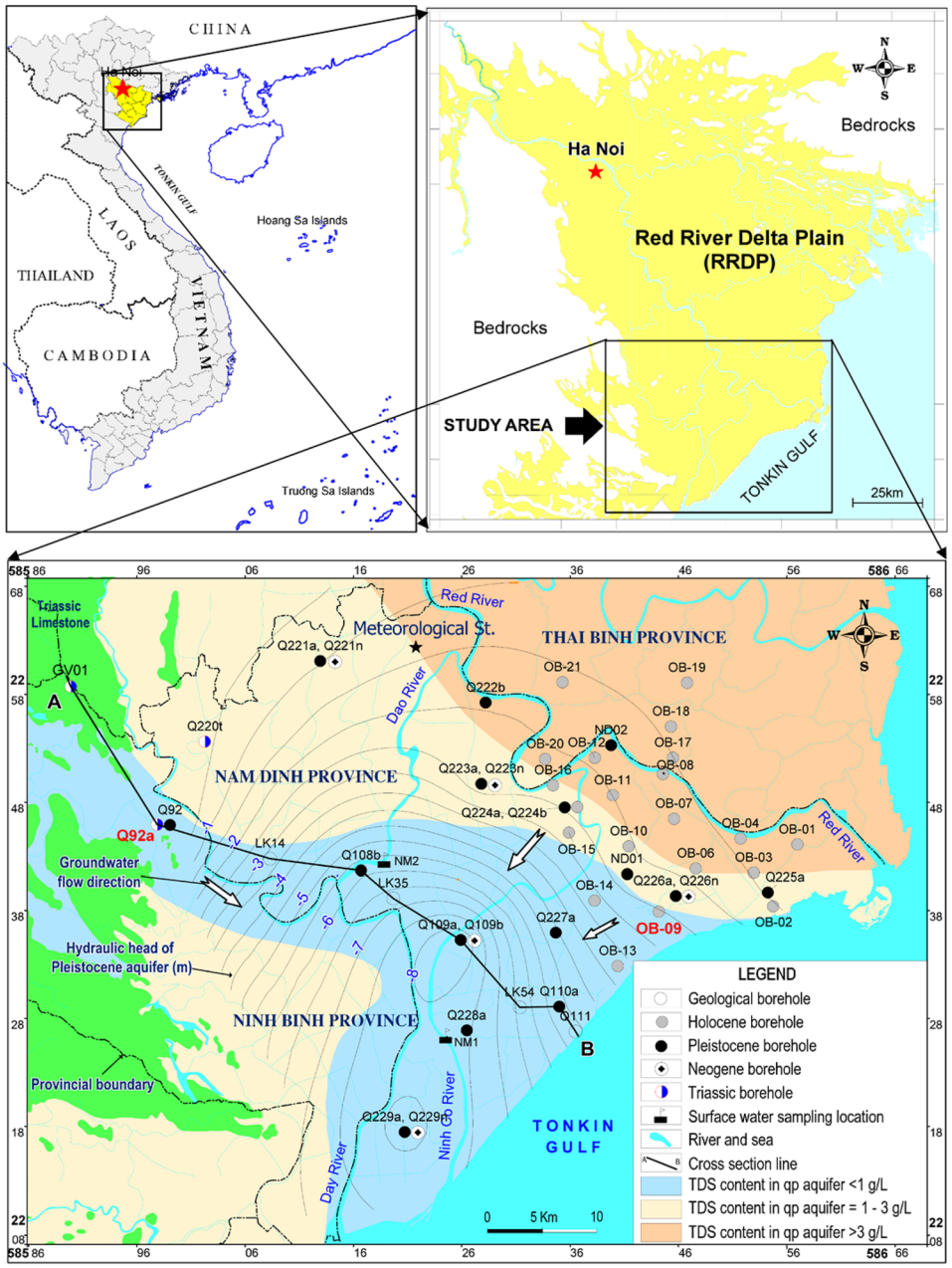
CHINA
Ha Noi
TONKIN GULF
LAOS
THAILAND
VIETNAM
CAMBODIA
Hoang Sa Islands
Truong Sa Islands
Bedrocks
Ha Noi
Red River Delta Plain
(RRDP)
Bedrocks
STUDY AREA
TONKIN GULF
25km
Triassic Limestone
GV01
A
Meteorological St.
Red River
THAI BINH PROVINCE
Q221a, Q221n
Q222b
Q220t
Dao River
NAM DINH PROVINCE
Q223a, Q223n
Q224a, Q224b
Q92
Q92a
LK14
Q108b
NM2
LK35
Groundwater flow direction
Hydraulic head of Pleistocene aquifer (m)
Q109a, Q109b
Q227a
OB-09
OB-13
LK54 Q110a
Q111
Q228a
NM1
NINH BINH PROVINCE
Provincial boundary
Q229a, Q229b
Ninh Co River
Day River
B
TONKIN GULF
0 5 Km 10
OB-21
OB-19
OB-18
OB-17
OB-08
OB-20 OB-12
ND02
OB-16
OB-11
OB-07
OB-04
OB-01
OB-10
OB-15
ND01
OB-06
OB-03
Q226a, Q226n
Q225a
OB-14
OB-02
Red River
LEGEND
Geological borehole
Holocene borehole
Pleistocene borehole
Neogene borehole
Triassic borehole
Surface water sampling location
River and sea
Cross section line
TDS content in qp aquifer <1 g/L
TDS content in qp aquifer = 1 - 3 g/L
TDS content in qp aquifer >3 g/L

(a)

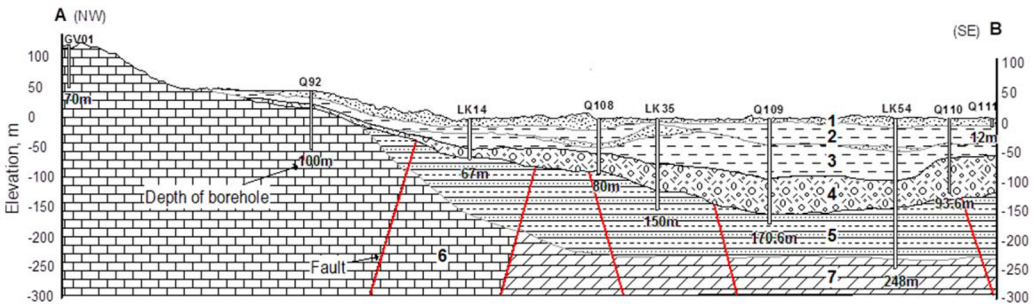
A (NW)
(SE) B
GV01
Q92
LK14
Q108
LK35
Q109
LK54
Q110
Q111
70m
100m
67m
80m
150m
170.6m
93.6m
12m
248m
Depth of borehole
Fault
Elevation, m
1
2
3
4
5
6
7

(b)

◂**Fig. 1** A map showing the study region: the Red River's Delta plain, Nam Dinh province, sampling locations, saline-brackish-fresh water boundary, and isolines of water hydraulic head of the groundwater in the Pleistocene aquifer (**a**). Geological setting of the study region drawn for the transect AB (**b**). See explanations for the sequence of the geological formation in the text

where $R_{2_{H,sample}}, R_{2_{H,std}}, R_{18_{O,sample}}, R_{18_{O,std}}$ are the isotopic ratios of [^{2}H]/[^{1}H], [^{18}O]/[^{16}O] in water samples and standards, respectively. The delta notation is expressed in per mil (‰). The standard used in these analyses is the Vienna Standard of Mean Ocean Water (VSMOW) supplied by the Isotopes Hydrology Laboratory of the International Atomic Energy Agency (IAEA IHL) based in Vienna, Austria.

The water isotopic compositions (δ^2H and δ^{18}O) could be positive or negative. Positive δ^2H and δ^{18}O mean that heavy isotopes present in water were enriched compared to the standard. On the contrary, negative δ^2H and δ^{18}O indicate more depletion of the heavy isotopes in study water compared to those in the standard. The extent of the enrichment or depletion of the ^{2}H and ^{18}O depends on a number of factors such as the atmospheric temperature, altitude, season, etc. The gradient of δ^{18}O by altitude was reportedly to range from − 0.25 to − 0.3‰ per 100-m rise (Clark et al. 1982; Erickson 1983). This data was used to determine the recharge area of groundwater in this study.

By the definition (Eqs. 1 and 2) the δ^2H and δ^{18}O in the seawater should be close to 0. Under the equilibration between evaporation-condensation-rainfall the relationship of δ^2H vs. δ^{18}O for the precipitation at the global scale will follow a so called Global Meteorological Water Line (GMWL) (Craig 1961):

$$\delta^2H = 8 \times \delta^{18}O + 10\ (‰). \tag{3}$$

The slope and intercept of Eq. (3) are much dependent upon the conditions under which the water was yielded. This is the principle of the isotopic approach in assessing the genesis of different water types. As mentioned above, the pattern of the Water Line is dependent on the climate and geographical conditions, so to assess the origin of the groundwater using water isotopic signatures (δ^2H and δ^{18}O) one needs to base on the regional meteoric water line (RMWL) instead of the GMWL. Groundwater which has its isotopic compositions positioning closely to the RMWL, i.e., the slope and intercept are similar to those of the RMWL, should have their origin from local precipitation. If the slope of the δ^2H vs. δ^{18}O relationship were lower than the slope of the RMWL and this relationship has two end-points, one at the position of seawater and another at the RMWL then the groundwater should be a mixture of local precipitation and seawater, i.e., seawater intrusion. If the isotopic signatures of groundwater position below and connect to the RMWL then the water should be a mixture of paleo-water with a long residence time or connate and local precipitation. The approach for assessing the genesis of groundwater was described in detail in, e.g., Clark and Fritz (1997) and Mook (2001).

Naturally, the mineralization of carbonaceous compounds in groundwater will accompany with the carbon-isotope discrimination in which the carbon-13 (^{13}C) composition will be depleted in the products thus it will be enriched in the reactants. For example, the ^{13}C-composition in the bicarbonate resulting from the dissolution of calcareous minerals should be more depleted compared to that composition in the carbonate residue. The extent of the carbon isotope discrimination in the processes in which carbon participates is expressed in the delta notation (δ^{13}C), similar to the water stable isotopes:

$$\delta^{13}C = \left(\frac{R_{13_{C,sample}}}{R_{13_{C,std}}} - 1 \right) \times 1000, \tag{4}$$

where $R_{13_{C,sample}}$, and $R_{13_{C,std}}$ stand for the isotopic ratio of [^{13}C]/[^{12}C] in the sample being measured and in the standard, respectively. The standard used in the δ^{13}C determination is VPDB (Vienna PeeDee Belemnite), it is a marine carbonate mineral of the PeeDee formation from the Cretaceous age taken from South Carolina (USA) and supplied by the IAEA IHL in Vienna, Austria.

By definition (Eq. 4) the DIC derived from the dissolution of inorganic calcareous minerals should have $\delta^{13}C_{DIC}$ close to 0, but the ^{13}C composition in DIC derived from mineralization of OM presented in aquifer deposits should be much depleted. This is because the ^{13}C composition in C3 terrestrial plants that are dominant in tropical regions like in Vietnam, was reported to be in the range of − 20‰ to − 35‰ vs. VPDB (Koln 2010). Hence, using the carbon-13 signature (δ^{13}C) in DIC one could assess the type of mineralization of groundwater during its seepage within aquifer as mentioned early (Clark and Fritz 1997).

Sampling procedure and field measurement

Nineteen (19) groundwater samples from the Holocene, sixteen (16) samples from Pleistocene, six (6) samples from Neogene, three (3) samples from Triassic aquifers and two (2) surface water (NM) samples from Dao and Ninh Co River (Online Appendix 1) were taken during rainy (Aug 2011) and dry (Mar 2012) seasons using a submersible pump, a Grundfos MP1. Sampling locations for Holocene aquifer were marked with symbol OB in the region adjacent to the Red River as shown in Fig. 1a. The sampling locations for the Pleistocene, Neogene and Triassic aquifers are shown

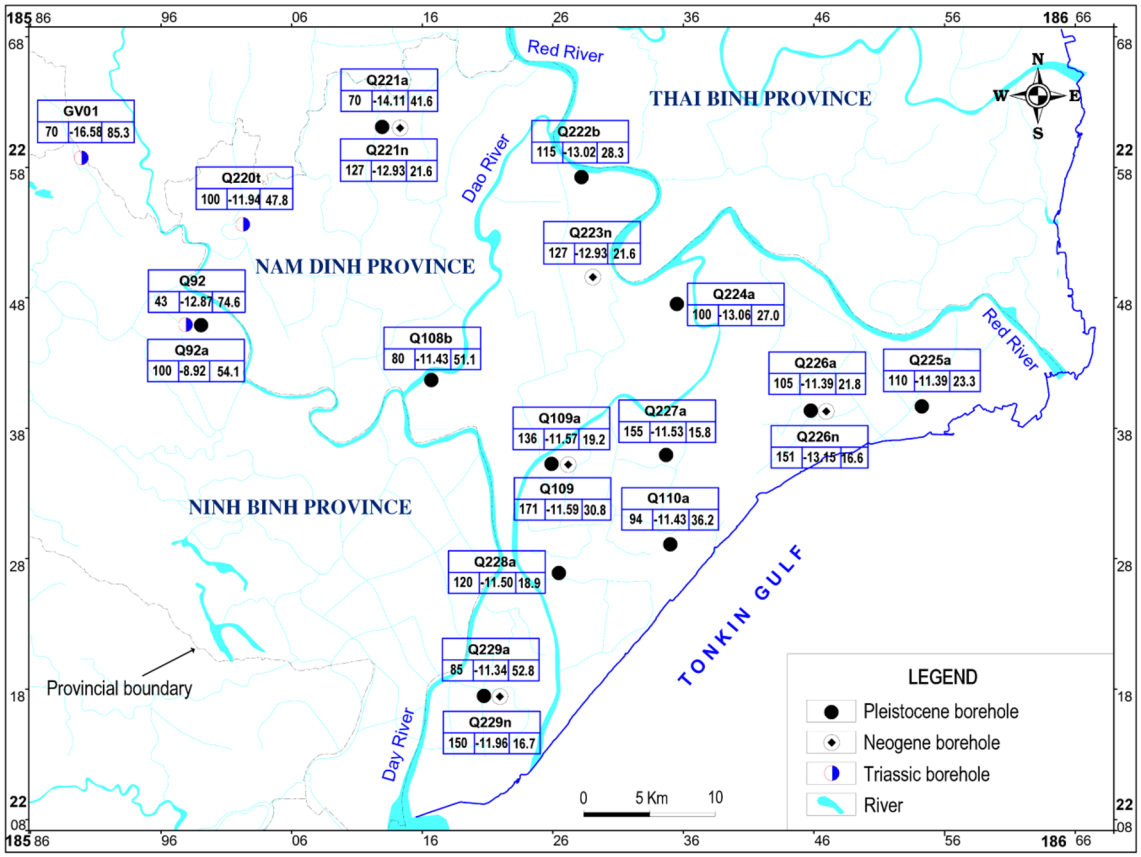

Fig. 2 Sampling locations of the groundwater from the Pleistocene, Neogene and Triassic aquifers along with information related to boreholes and water in the boreholes. **a** Borehole ID (Q stands for boreholes of the National Groundwater Monitoring Network with a sequence number in the Network; Characters a or b, n and t standing aside the borehole ID indicate the Pleistocene, Neogene and Triassic aquifers, respectively); **b** borehole depth (meter from the ground surface); **c** ^{13}C-isotopic composition in DIC (‰ vs. VPDB); **d** ^{14}C content in DIC (pMC)

in Fig. 2 along with the depth of the boreholes, ^{13}C- and ^{14}C-contents in groundwater from those boreholes.

Before taking groundwater samples, water table level in each sampling location was first measured using a logger system then the stagnant water in the wells was completely flushed out by pumping it out till the pH and temperature of the water were unchanged. A flow cell equipped with probes for pH, temperature, and electrical conductivity (EC) was mounted directly on sampling tube. The measurements were carried out with a WTW Multi 197i multi-purpose instrument using a WTW Tetracon 96 EC probe and a WTW SenTix 41 pH electrode.

Alkalinity was determined shortly after sampling using the Gran-titration method (Stumm and Morgan 1981). Ferrous ion (Fe^{2+}) concentration in the water samples was determined by colorimetry using a Hach DR/2010 instrument and Ferrozine method (Stookey 1970). The dissolved inorganic carbon (DIC) including bicarbonate, carbonate ions and CO_2 dissolved in water, used to determine the content of carbon-13 and carbon-14 was precipitated in the form of $BaCO_3$ from around 100 liters of groundwater at pH 10 using saturated $BaCl_2$ solution and CO_2-free KOH (Merck, Germany).

Around 100 mL of groundwater were first filtered through 0.45 µm mesh polycarbonate membranes to remove suspended matters then split into two parts. One part was acidified with HNO_3 (65%, PA grade, Merck, Germany) to a pH of about 1–2. These samples were subject to the quantification of cations NH_4^+, Na^+, K^+, Ca^{2+} and Mg^{2+}. Another part was kept without acidification for Cl^-, NO_3^- and SO_4^{2-} determination. All samples were stored in bottles made from high density polyethylene (HDPE) resin and refrigerated until laboratory analysis.

Surface water from Dao and Ninh Co River (NM1 and NM2 sites, Fig. 1a) was collected the same day of groundwater sampling. The samples were taken at a depth of 0.5 m from surface and around 2 m apart from the bank of the rivers.

Rain water was collected monthly for the 2011–2012 years using a device constructed following an IAEA's recommendation (IAEA 2002). The device was

installed on the roof of the premises of the Meteorological Station (marked with a star in Fig. 1a) in the city of Nam Dinh.

Rain water, surface water and groundwater samples for stable isotopic composition determination were stored in 50 mL capacity double caps HDPE bottles.

For the tritium determination, in each sampling site 1 L of water was sampled into a HDPE bottle closed with a tight cap to avoid the isotopic exchange with atmospheric moisture. The samples were transferred to laboratory in Ha Noi for further treatment and measurement of tritium activity.

Samples' treatment in the laboratory and analytical procedure

The ionic content of water samples was quantified by ion chromatography method (IC) using a DIONEX 600 at the Institute for Nuclear Science and Technology (INST in Ha Noi). A quality control program was applied for the ionic content determination by analyzing standard solutions supplied by the IC supplier (DIONEX). The standard deviation of results derived by the laboratory was within ± 5% from the certified value for respective constituents.

The stable isotopes compositions of deuterium, oxygen-18 and carbon-13 (δ^2H, $\delta^{18}O$ and $\delta^{13}C$) were analyzed at the INST on an Isotope Ratio Mass-Spectrometer (IR MS, IsoPrime, GV, UK) equipped with an Elemental Analyzer (EA 3000, Eurovector, Italy).To analyze for $\delta^{13}C$, the barium carbonate precipitate was first washed off the excess of alkali by boiled deionized water till neutral pH was attained then freeze-dried. The dry and alkali-free carbonate barium was stored in HDPE vials till analysis. For the δ^2H and $\delta^{18}O$ analyses, the water samples collected and filtered in the field did not need any additional treatment in the laboratory.

Procedures applied for analyzing the stable isotopic compositions were implemented as per the supplier's manual and as follows.

For the δ^2H analysis 2 µL of water was injected into the EA where the sample was decomposed on the Ni-catalyst at 1050 °C to form hydrogen gas. A continuous flow of He-carrier gas carried the H_2 gas through a $Mg(ClO_4)_2$ moisture trap to dry then by passing through a chromatographic column to purify from contaminants before entering the ionization chamber of the IR MS where H_2 was ionized. The flow of He-carrier gas carried the H_2^+ ions into the mass separator of the IR MS where masses 2 ($^1H_2^+$) and 3 ($^1H^2H^+$) were separated from each other. The H_2^+ and H_3^+ ions were collected and counted by the respective Faraday cups installed on the exit from the separator.

For the $\delta^{18}O$ analysis, the decomposition of water was carried out in the EA on the glassy carbon catalyst at 1150 °C to form CO_2 gas. A continuous flow of He-carrier gas carried the CO_2 through a $Mg(ClO_4)_2$ moisture trap followed by the chromatographic purification before entering the ionization chamber to ionize the CO_2 gas. The carrier gas carried the ions of masses 44 ($^{12}C^{16}O_2^+$) and 46 ($^{12}C^{16}O^{18}O^+$) into the mass separator of the IR MS where they were separated from each other. Ions $^{12}C^{16}O_2^+$ and $^{12}C^{16}O^{18}O^+$ were collected and counted by the respective Faraday cups installed on the exit from the separator.

For the $\delta^{13}C$ analysis, around 100 µg of the freeze-dried $BaCO_3$ was wrapped in tin capsules and subjected to decomposition at 1050 °C on the chromium oxide catalyst in the EA of the IR MS to form CO gas. The formed CO was carried by a continuous flow of He-carrier gas through a chromatographic column to purify from contaminants before entering the ionization chamber to ionize. A flow of the carrier gas carried the ions of masses 28 ($^{12}C^{16}O^+$) and 29 ($^{13}C^{16}O^+$) into the mass separator of the IR MS where they were separated from each other. The ions $^{12}C^{16}O^+$ and $^{13}C^{16}O^+$ were collected and counted by the respective Faraday cups installed on the exit from separator.

The isotopic ratio analyses were carried out in parallel for samples and the standard under the same decomposition conditions. The MassLynx software was used to calculate the ratios of deuterium content ([$^1H^2H$]) to those of protium ([$^1H_2$]), i.e., R_{2_H} for the sample and the standard based on the areas of the mass peaks 3 and those of 2. The δ^2H was then calculated by the same Mass Lynn software based on Eq. (1). Similarly, the $\delta^{18}O$ and $\delta^{13}C$ were derived from the ratios of the areas of the masses peaks 46–44 and 29–28 for the sample and standard (Eqs. 2 and 4), respectively. The precision of δ^2H determination was ± 2‰ and that of $\delta^{18}O$ and $\delta^{13}C$ was ± 0.2‰.

For tritium measurement, water samples were first subjected to distillation to remove the minerals dissolved till EC was less than 10 µS cm^{-1}. Around 500 mL of the distilled water samples were then subjected to the electrolytic enrichment for tritium at 4 °C till around 10 mL was attained (Villa and Manjon 2004; Plastino et al. 2007). The tritium enriched water samples were purified again by distillation and then mixed with the low tritium Ultima Gold scintillation cocktail (Hewlett–Packard, HP Supplier) in vials of 20 mL capacity to count for the ^3H activity on a low background HP Liquid Scintillation Counter TriCarb TR 3700. The ^3H activity in water was expressed in the Tritium Unit (TU, 1 TU = 0.118 Bq L^{-1}). The limit of quantification (LOQ) for ^3H was estimated to be as low as 0.4 TU. The accuracy of the determination was validated by our participation in the inter-comparison exercises of the TRI-2004 and TRI-2008 organized by the IAEA IHL in the years 2004 and 2008. In the 2004 exercise, the Hanoi laboratory (no. 74) produced results having Z scores of − 1.25 and 0.59 for the samples of 1.74 TU and 5.43 TU, respectively. In the 2008 exercise, the laboratory (no. 27) produced results with Z scores of 0.42

and 1.57 for the samples of 4.07 TU and 1.54 TU, respectively (Groening et al. 2004, 2008).

The ^{14}C-analysis was conducted at the Center for Nuclear Techniques in the city of Ho Chi Minh (HCM) where $BaCO_3$ was decomposed by concentrated H_3PO_4 (PA grade, Merck supplier) to obtain CO_2 for further benzene synthesis (Noakes et al. 1967; Tamers 1975; Gupta and Polach 1985). The benzene obtained was mixed with the Ultima Gold scintillation cocktail (HP Supplier) in vials of 20 mL capacity, and then counted for the ^{14}C activity on the HP LSC TriCarb TR 3770.

Groundwater residence time (the ^{14}C-age) estimation

As mentioned earlier, the aim of groundwater age determination is to verify follow pattern and to estimate its flow rate. To have an acceptable age estimation certainty using the ^{14}C-dating method, particularly for groundwater in which the absolute ^{14}C-activity is usually very low, the ^{14}C-activity in samples must be measured relative to a standard under the same conditions. The result of this measurement is expressed in percent of the modern carbon (pMC) as follows:

$$^{14}a = \frac{^{14}A_{\text{sample}}}{^{14}A_{\text{std}}} \times 100\ (\text{pMC}), \tag{5}$$

where ^{14}a is the relative ^{14}C-activity or the ^{14}C-content; $^{14}A_{\text{sample}}$ and $^{14}A_{\text{std}}$ are the absolute activities (Bq g^{-1} C) of ^{14}C in the sample and standard, respectively.

The standard used in this study was oxalic acid II (ox-II) made from French beet molasses planted in 1977 and supplied by the National Institute of Standards and Technology (NIST, USA), which has a ^{14}C-activity of 0.2147 Bq g^{-1} C and $\delta^{13}C = -25‰$ (Mann 1983).

The groundwater age calculation was made based on the data of the ^{14}C-content in the DIC as follows:

$$^{14}t = 8268 \ln \frac{^{14}a^0_{\text{in}}}{^{14}a_{\text{sample}}} (\text{a BP}). \tag{6}$$

Equation (6) was derived from the law of the ^{14}C radioactive decay, where ^{14}t denotes the age in years Before Present (BP), of a groundwater sample estimated by the ^{14}C-content in the DIC; the number 8268 is quotient of half-life of ^{14}C-isotope (5700 a) to ln2; $^{14}a^0_{\text{in}}$ is the initial ^{14}C-content in the DIC before entering the saturated zone (pMC), and $^{14}a_{\text{sample}}$ is the ^{14}C-content (pMC) in the DIC of the sample to be measured. The term "Before Present" implies the age relative to the time when the standard was produced. If the $^{14}a_{\text{sample}}$ is close to 100% groundwater would be assumed to be "modern".

The groundwater age estimation by Eq. (6) requires corrections for the $^{14}a^0_{\text{in}}$ because in the unsaturated zone, the carbon present in the DIC would participate in the isotopic exchange with the modern carbon from the biogenic CO_2 which is released from the plants' roots respiration on one hand, and on the other hand, a new portion of bicarbonate could be formed there due to the oxidation of OM and the dissolution of inorganic, "dead" calcite and/or dolomite minerals present in the soil or sediment. In the dissolution process the biogenic CO_2 is the key reactant. All these processes could modify the value of $^{14}a^0_{\text{in}}$. To do the correction for the $^{14}a^0_{\text{in}}$, an isotope mixing model referred to as the model of complete exchange with CO_2 in the unsaturated zone proposed by Gonfiantini (Salem et al. 1980) for a closed/confined system was applied as follows:

$$^{14}a^0_{\text{in}} = \frac{\delta^{13}C_{\text{DIC}} - \delta^{13}C_{\text{cc}}}{\delta^{13}C_{CO_{2,\text{org}}} - \delta^{13}C_{\text{cc}} + \varepsilon_{CO_2/\text{DIC}}}, \tag{7}$$

where $\delta^{13}C_{\text{DIC}}$, $\delta^{13}C_{\text{cc}}$, $\delta^{13}C_{CO_{2,\text{org}}}$ are the carbon-13 compositions, respectively, in the DIC in a groundwater sample, in calcareous materials in soil/sediment and in the biogenic dioxide originated from the decomposition of organic matters; $\varepsilon_{CO_2/\text{DIC}}$ is the fractionation coefficient for ^{13}C in the isotopic exchange reaction between the biogenic carbon dioxide and DIC which is temperature dependent (Bigeleisen and Mayer 1947; Mook et al. 1974):

$$\varepsilon_{CO_2/\text{DIC}} = \left(-\frac{9483}{T} + 23.89\right)‰, \tag{8}$$

where T is the temperature of the groundwater sample, in Kelvin.

In the study area the $\delta^{13}C_{\text{cc}}$ in soil was found to be ranging from 1 to 2‰ with an average value of 1.5‰ was taken to correct for $^{14}a^0_{\text{in}}$. The $\delta^{13}C_{CO_{2,\text{org}}}$ in Eq. (7) was taken as high as −23‰, as it is characterized for carbon dioxide generated from mineralization of remnants of C3 plants in tropical areas followed by its diffusion to aquifer (Appelo and Postma 2007).

Detail of the procedure for $^{14}a^0_{\text{in}}$ calculation could be found in Fontes and Garnier (1979) and Fontes (1983). The computer code NETPATH (Plummer et al. 1994) was used for this correction. The data of ^3H activity were used to confirm whether the study water sample was old or modern.

Results

The concentrations of major ionic constituents dissolved in groundwater samples taken in August 2011 (rainy season, RS) and in March 2012 (dry season, DS) from the Holocene,

Pleistocene, Neogene and Triassic aquifers are presented in Online Appendix 1. The isotopic composition of deuterium (δ^2H), oxygen-18 ($\delta^{18}O$) as well as tritium activity in water, and the content of carbon-13 ($\delta^{13}C$) and carbon-14 in the DIC are presented in Online Appendix 2 (Online Appendices 1 and 2 are available separately as supplement materials).

Groundwater chemistry

Groundwater in the study region could be divided into three types based on its total dissolved solids (TDS) content. In the NE area groundwater was found of two types. In Thai Binh province and northernmost part of Nam Dinh province (Fig. 1a), the groundwater in all Holocene, Pleistocene, Neogene and Triassic aquifers is saline with TDS > 3 g L^{-1} but in a part of the northern Nam Dinh province lying along the Red River (Fig. 1a), groundwater in these aquifers is brackish with TDS ranging from 1 to 3 g L^{-1}. In the SW area, the southern part of Nam Dinh and northern part of Ninh Binh province (Fig. 1a), groundwater in the deep aquifers is fresh containing TDS < 1 g L^{-1}. The fresh-brackish and brackish-saline water boundaries drawn based on the TDS content in the deep aquifers' groundwater of the study region is presented in Fig. 1a. The blue, light brown and dark brown color in Fig. 1a indicate the areas of fresh, brackish and saline waters, respectively. Brackish water in the deep aquifers in the NE area seems to be resulting from the migration of saline water from the NE or/and from the diffusion downwards of saline water from the upper aquitard due to the high rate of fresh water mining in the SW and this will be discussed later on.

The chemical types of groundwater in aquifers were identified by building Piper diagrams, the same approach used by Nguyen et al. (2014) to differentiate types of groundwater in the entire RRDP. Because of the lack of isotopic data for discussing the genesis of brackish groundwater in the southern part of Ninh Binh province (the area with light brown color in the southern part of Ninh Binh province, Fig. 1a), our discussion thereinafter will be focusing on the NE and SW excluding the southern part of Ninh Binh province.

The Piper diagrams showing the chemical types of the groundwater in Holocene, Pleistocene, Neogene and Triassic aquifers in the study region are presented in Fig. 3a, b, respectively, for the NE and SW areas during the rainy season. The chemistry of the groundwater in the study region was almost the same during the dry and rainy seasons (Online Appendix 1).

As seen from Fig. 3a in the NE area, water tapped from the Holocene aquifer is saline of Na–Cl type, with the exception of borehole OB-09 where water is pure Na–HCO_3 type (Fig. 3a). In the same region, water tapped from Pleistocene and Neogene aquifers is a mixture of Na–Cl type and fresh Ca–HCO_3 type, i.e., Na–Ca–Cl–HCO_3 type, but the contribution of the Na–Cl type is dominant, e.g., water in the Q224a and Q226a or Q221n boreholes (Fig. 3a, see Fig. 2 for locations). The reason why water in the OB-09 site is fresh will be discussed in more detail in the Discussion Part.

Contrary to the NE, in the SW area the groundwater from Pleistocene, Neogene and Triassic aquifers is of Na–Ca–HCO_3 type, except for those in the borehole Q92a in which the water is a mixture of chloride and bicarbonate types (Fig. 3b).

Figure 4 depicts the distribution of electron donor ions Fe^{2+}, Mn^{2+}, NH_4^+, and acceptors ions H^+, NO_3^-, and SO_4^{2-} in the groundwater within the Holocene aquifer. Figure 5 shows the same distribution within Pleistocene aquifer. As seen from Figs. 4 and 5, the pH of the groundwater was buffered, ranging from 7.40 to 7.65 and from 7.14 to 7.40, respectively, in the Holocene and Pleistocene aquifers. The concentration of sulphate ion in Holocene aquifer was rather low (from around 0.03 mmol L^{-1} to 0.08 mmol L^{-1}) unlike that, seawater having a high SO_4^{2-} concentration (29 mmol L^{-1}) was conservatively mixing with fresh water in shallow aquifer. Ammonia concentration in the groundwater from Holocene aquifer ranges from 1.40 to 4.20 mmol L^{-1} whereas it is lower, from 0.22 to 1.44 mmol L^{-1}, in water of the Pleistocene aquifer. The concentration of ferrous ions in groundwater in both aquifers was low (Figs. 4, 5).

In the Holocene and Pleistocene aquifers the following chemical reactions could proceed.

(a) Calcite dissolution to form bicarbonate

$$CO_2 + H_2O + CaCO_3 \rightarrow Ca^{2+} + 2HCO_3^-. \quad (9)$$

The carbon dioxide source for reaction (9) is primarily coming from plants' root respiration (Fontes 1983).

(b) Incongruent dissolution of biogenic high Mg-calcite: This mineral is frequently found in the aquifer sediments of Quaternary deltas in tropical regions and the dissolution process can be expected as follows (Appelo and Postma 2007):

$$Ca_{1-x}Mg_xCO_3 \rightarrow a \cdot Ca_{1-y}Mg_yCO_3 + (x - ay) \cdot Mg^{2+} + (1 - x - a + ay) \cdot Ca^{2+} + (1 - a) \cdot CO_3^{2-}. \quad (10)$$

The incongruent dissolution of the Mg-calcite (reaction 10) probably occurs easily in the aquifers following the organic matters oxidation (reaction 11) by which ion protonium was formed.

(c) Reduction of sulphate by organic matters:

$$2CH_2O + SO_4^{2-} \rightarrow H_2S + 2HCO_3^- \rightarrow H^+ + HS^- + 2HCO_3^-. \quad (11)$$

(d) Reduction of iron-oxyhydroxide by organic matters:

$$CH_2O + 4FeOOH + 7H^+ \rightarrow 4Fe^{2+} + HCO_3^- + 6H_2O. \quad (12)$$

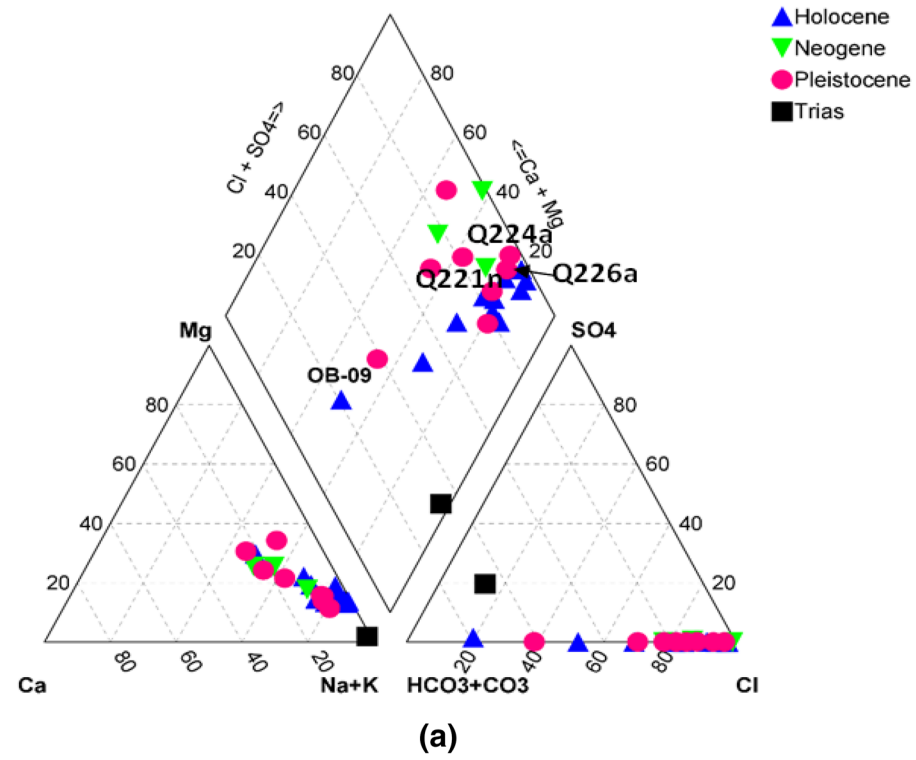

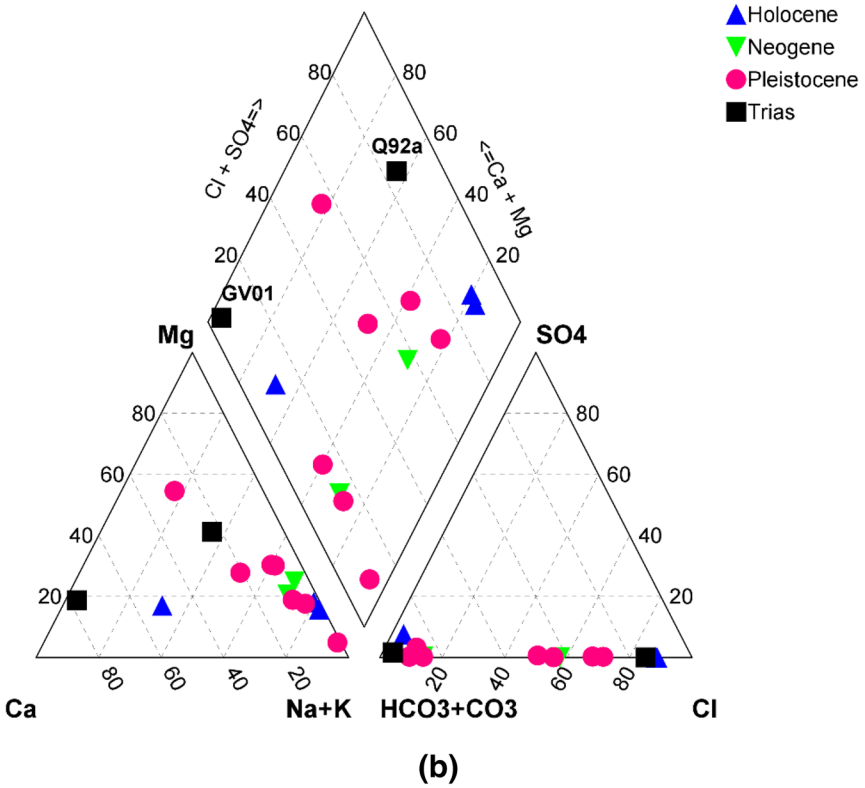

Fig. 3 Piper diagrams showing the types of water in the Holocene, Pleistocene, Neogene and Triassic aquifers in the NE (**a**) and in the SW Nam Dinh (**b**) during the rainy season

(e) Biological ammonification of nitrate:

$$NO_3^- + 10H^+ + \text{enzyme} \rightarrow NH_4^+ + 3H_2O. \quad (13)$$

Reactions (9) though (13) buffered the groundwater pH and lowered the sulphate concentration in the water as it was found in this study during both rainy and dry seasons (Online Appendix 1).

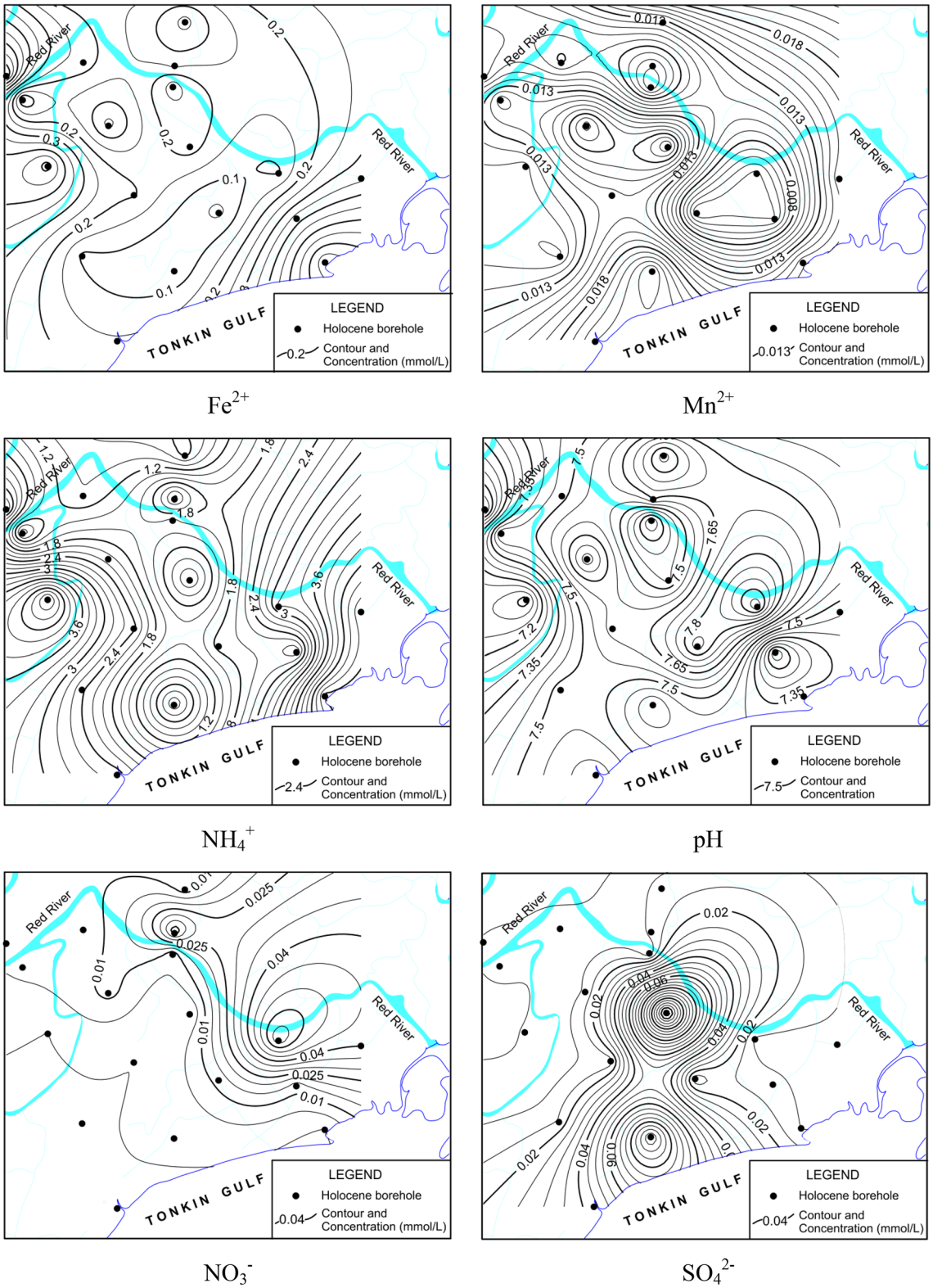

Fig. 4 Distribution of electron donors (NH_4^+, Mn^{2+}, Fe^{2+}) and electron acceptors (H^+, SO_4^{2-}, NO_3^-) concentration (mmol L^{-1}) in water of the Holocene aquifer within the study region

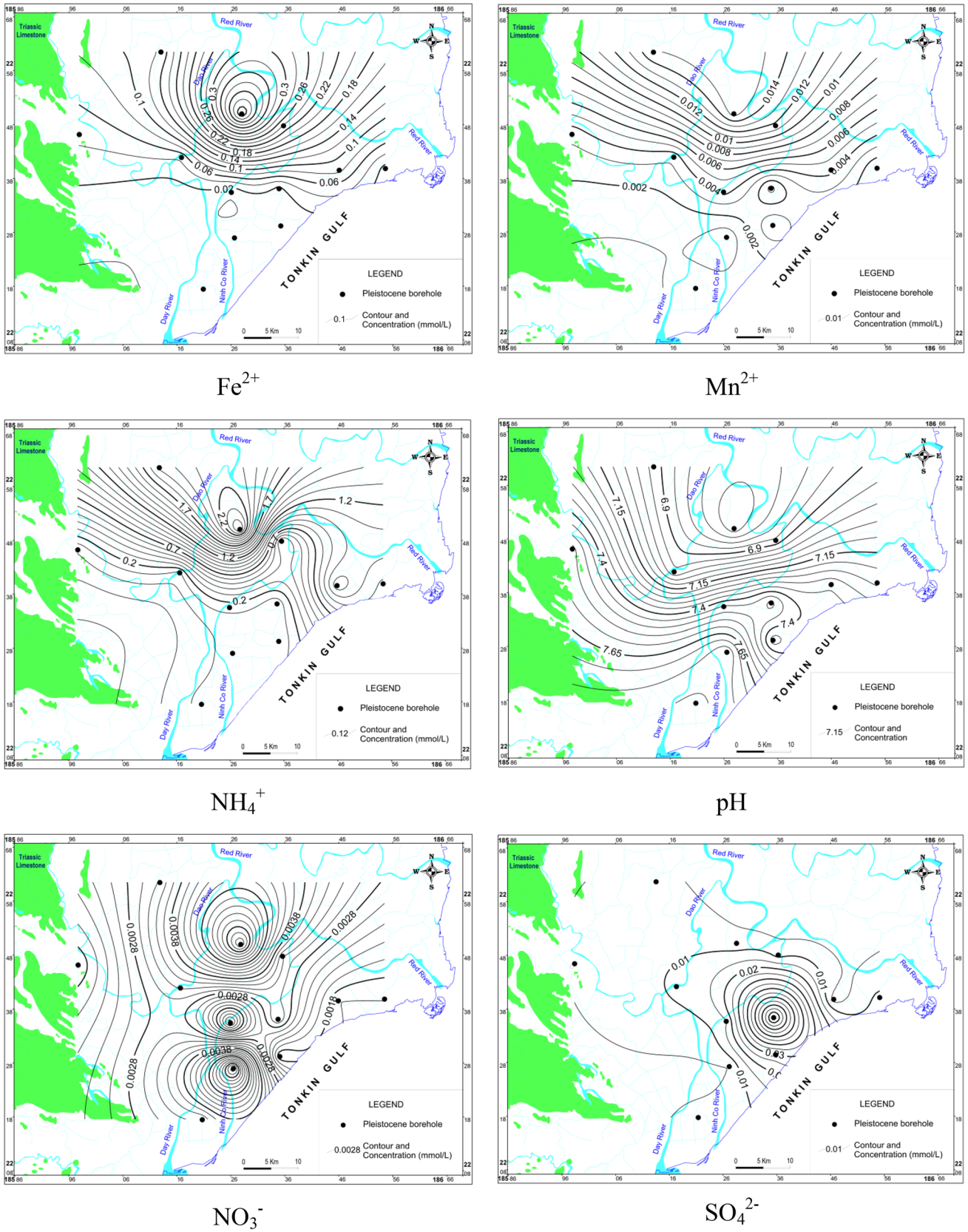

Fig. 5 Distribution of electron donors (NH_4^+, Mn^{2+}, Fe^{2+}) and electron acceptors (H^+, SO_4^{2-}, NO_3^-) concentrations (mmol L^{-1}) in water of the Pleistocene aquifer within the study region

Residence time (age) of groundwater in the aquifers

Tritium activity in the groundwater from Holocene aquifer was comparable with the surface water ranging from 2.0 to 3.0 TU (Online Appendix 2). However, the tritium content in the groundwater from Pleistocene, Neogene and Triassic aquifers was lower than LOQ of determination of 0.4 TU. This finding reflects the fact that groundwater in Holocene aquifer is modern and that it is continuously recharged from surface water. This was confirmed by the ^{14}C-age of water from wells OB-10 and OB-12 for which the ^{14}C-content was 101.2 pMC and 103.5 pMC, respectively (Appen. 2). In contrast, groundwater in Pleistocene, Neogene and Triassic aquifers did not receive recent recharge, therefore it was of an older age, e.g., water in borehole Q223n made into Neogene aquifer has a ^{14}C-age as old as 14.5 ka BP (Online Appendix 2).

Results of ^{14}C-dating revealed that along transect AB (Fig. 1a) groundwater in borehole GV01 is modern (i.e., recent precipitations), while in the Pleistocene aquifer it was 1.1 ka old at borehole Q92, 3.3 ka old in Q108 and 11.3 ka old in borehole Q109 (Fig. 6). However, the age of groundwater found in Q110a borehole installed behind borehole Q109 at the sea coast decreased down to 6 ka (Fig. 6 and Online Appendix 2).

Groundwater isotopic composition

Figure 7a, b depicts the regional meteoric water line (RMWL) determined for study region during 2011–2012 period along with isotopic compositions in groundwater collected during the rainy (RS) and dry (DS) seasons from Holocene (Fig. 7a), Pleistocene, Neogene and Triassic aquifers (Fig. 7b), respectively. The RMWL was constructed based on the isotopic compositions of precipitations collected monthly for 1 meteorological year, beginning in Aug 2011 to the end of Jul 2012.

The RMWL in the study region follows a model described by the equation (Fig. 7a, b):

$$\delta^2\mathrm{H} = 8.48 \times \delta^{18}\mathrm{O} + 15.88 \ (R^2 = 0.99). \quad (14)$$

The slope and intercept of the RMWL in region (Eq. 14) was a little higher than those of the Global Meteoric Water Line of, respectively, 8 and 10, probably due to the kinetic effect during rain fall in the tropical regions where atmospheric temperatures are usually high (Clark and Fritz 1997).

The open and solid red color circles in Fig. 7b represent isotopic composition in water collected in the RS and DS from borehole GV01 installed in Gia Vien district, Ninh Binh province. Though the borehole was made into Triassic limestone bedrock (Fig. 1b) water in it characterizes the local and modern precipitations with its isotopic composition positioned close to the RMWL (Fig. 7b), it contains (85.30 ± 0.87) pMC and 2.03 TU (Online Appendix 2), i.e., comparable with the average tritium activity found year round in precipitations in the Red River Delta region (Nhan et al. 2013).

Results of water stable isotopic composition in the studied groundwater revealed that the water in Holocene aquifer was a mixture of surface and seawater (Fig. 7a), but water in the Pleistocene, Neogene and Triassic aquifers was a mixture of paleo-water and modern precipitations (Fig. 7b). Here, the paleo-water must be understood as groundwater having along transit time (age), up to several thousand years.

Discussion

Genesis of groundwater resources in the southern part of Red River's Delta plain

Groundwater in Holocene aquifer is a mixture of three end-members, namely: local precipitations, water from Red River and seawater. The three end-members mixing character of water in Holocene aquifer is clearly demonstrated in Fig. 8,

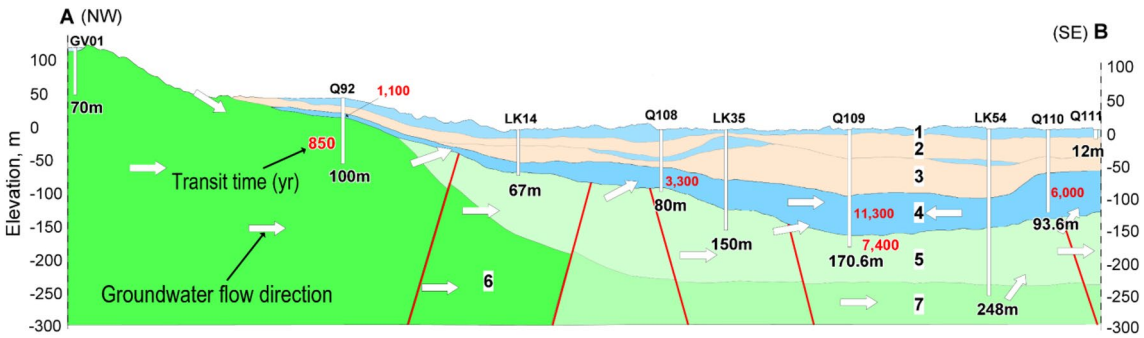

Fig. 6 The ^{14}C-ages and conceptual model indicating the flow directions of the groundwater in the Pleistocene, Neogene and Triassic aquifers in the study region

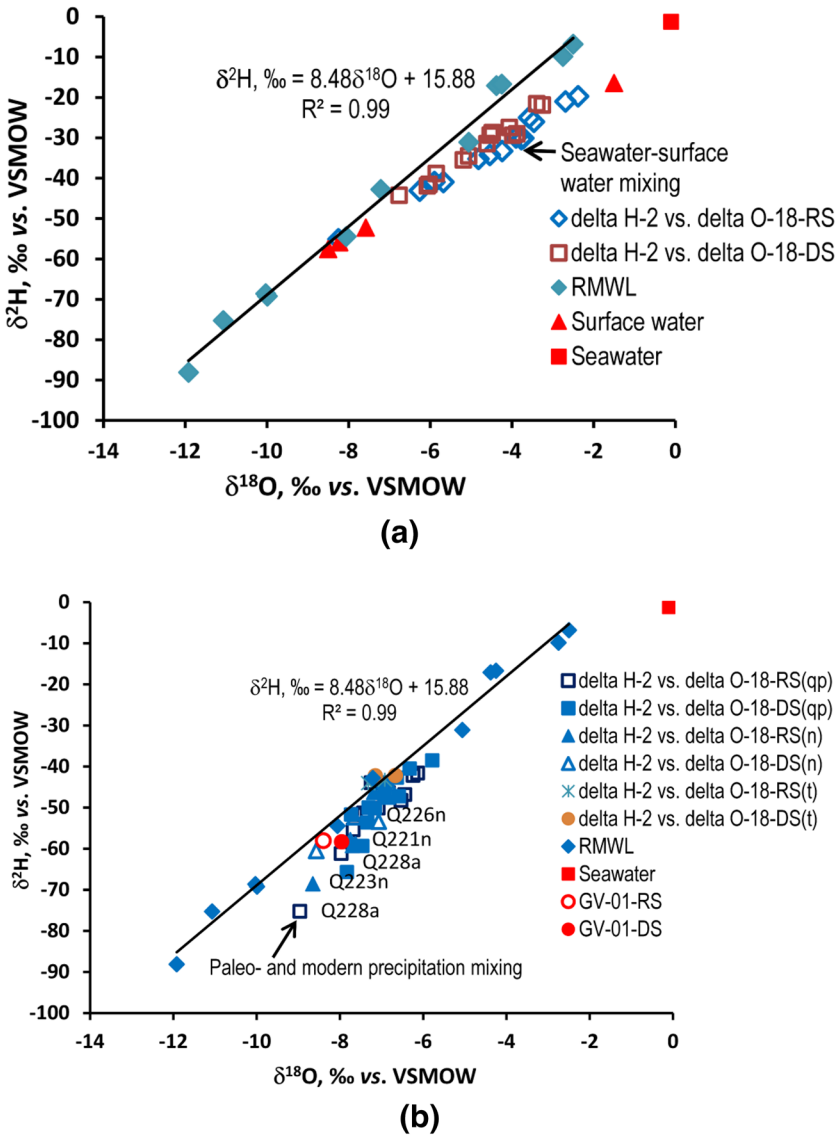

Fig. 7 Isotopic compositions in the groundwater from the Holocene aquifer (**a**) and from the Pleistocene, Neogene and Triassic aquifers (**b**) plotted with the RMWL for the study region. By isotopic compositions, the groundwater in the Holocene aquifer appears to be mixing between surface water and seawater, yet water in the Pleistocene, Neogene and Triassic aquifers represent a mixing between young age precipitations and paleo-water

where the relationship of $\delta^{18}O$ vs. chloride concentration ($[Cl^-]$) in water was arranged within a triangle with the three apexes representing the local precipitations, Red River's water and seawater (Fig. 8).

Let the contribution of precipitation's water to groundwater in Holocene aquifer be x, the River's be y and seawater be z, then one could compute x, y and z for each water sample based on $\delta^{18}O$, and $[Cl^-]$ using three end-members model (Stiefel et al. 2009) as follows:

$$x + y + z = 1, \tag{15}$$

$$x \times \delta^{18}O_p + y \times \delta^{18}O_r + z \times \delta^{18}O_s = \delta^{18}O_{gw}, \tag{16}$$

$$x \times [Cl^-]_p + y \times [Cl^-]_r + z \times [Cl^-]_s = [Cl^-]_{gw}, \tag{17}$$

where subscripts p, r, s, and gw denote the precipitations, river's, seawater and groundwater, respectively.

Table 1 shows the results of estimated contribution (in percent) by local precipitations, river's water and seawater to groundwater in different boreholes made into Holocene aquifer in the study region during the RS and DS. This estimate was made based on the average $\delta^{18}O_p$, $\delta^{18}O_r$ and $\delta^{18}O_s$ of $-8.40‰$, $-4.0‰$ and $-0.1‰$ (vs. VSMOW), and $[Cl^-]_p$, $[Cl^-]_r$, and $[Cl^-]_s$ of 0.10 mmol L^{-1}; 0.11 mmol L^{-1} and 566 mmol L^{-1}, respectively. The data of $\delta^{18}O_p$, $\delta^{18}O_r$, $[Cl^-]_p$, and $[Cl^-]_r$ for precipitations and Red River's water in the RRDP were from Nguyen (2009). The $[Cl^-]_{gr}$ and $\delta^{18}O_{gr}$ were taken from Online Appendixes 1 and 2, respectively. Here, the river's water must be included as well as water from irrigation canals in the region because this system is directly connected to Red River via Dao and Ninh Co tributaries (Fig. 1a).

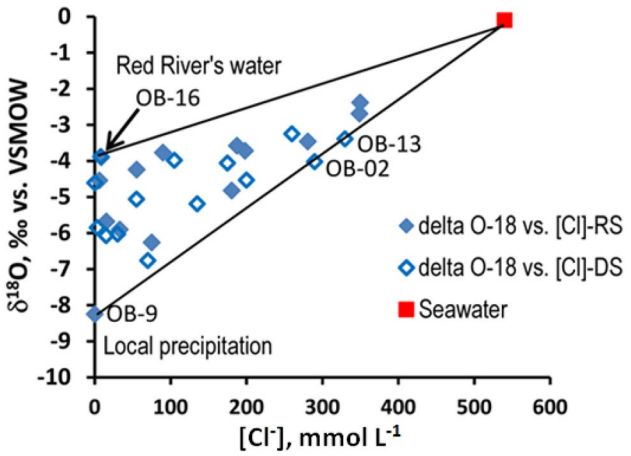

Fig. 8 The $\delta^{18}O$ vs. molar [Cl^-] relationship for groundwater in the Holocene aquifer in the study region representing a mixture of three end-members: local precipitations, Red River's water and seawater (see Fig. 1a for OB-09, OB-16, OB-02 and OB-13 locations)

As seen from Table 1, groundwater from boreholes located deep inland, e.g., OB-07, OB-08, OB-12, and OB-16 (see Fig. 1a for locations) has low contribution of seawater. This contribution was only from 0.4 to 5.5% in the RS and from 1.1 to 6.1% in DS. However, waters from boreholes nearby the River's mouth and coastline do have a high contribution of seawater. Water from the OB-01 and OB-04 boreholes installed close to the Red River's mouth contains, respectively, 37% and 61% seawater in the RS and 37% and 65% seawater in the DS (Table 1). Borehole OB-01 is about 500 m from the River's bank, while OB-04 is installed right on the River's bank. Apparently, seawater intruded the Holocene aquifer via the River. Active sand excavation (for construction purposes) from the River's bed combined with construction of upstream hydroelectric reservoirs, reduce downstream sediments deposits; the combination of these factors could much facilitate seawater to intrude deep inland and to diffuse to the aquifers. Boreholes OB-02 and OB-13 are located at 50 and 100-m from the sea shore (Fig. 1a) so apparently groundwater around these locations could be directly affected by seawater intrusion.

From Table 1 one can see that groundwater from borehole OB-9 was fresh with no seawater detected. The chloride concentration and the $\delta^{18}O$ in the groundwater from borehole OB-09 were 0.10 mmol L^{-1} and −8.25‰, respectively (Online Appendices 1 and 2) that almost coincided with the [Cl^-] and heavy oxygen isotope signature found in local precipitations. This supports the rainwater origin of groundwater around OB-09 borehole. In fact, borehole OB-09 is located in a lower area of the Giao Thuy district that is capable of storing rain water year round making rain water to be the most dominant source recharging shallow aquifer. On the other hand, the aquifer sediment around borehole OB-09 is purely coarse sand so the chemistry of groundwater in this area is mainly dependent upon the chemistry of the local precipitations.

Similarly to Holocene aquifer, groundwater in Pleistocene and Neogene aquifers in the NE area is brackish and saline. The EC and [Cl^-] in water from boreholes Q221a, Q222b, Q224a, Q225a, Q226a, Q221n, Q223n and Q226n range from 2540 to 6980 µS cm^{-1} and from 22 to 63 mmol L^{-1}, respectively, in the RS and DS (Online Appendix 1). Water from these boreholes contains also an elevated concentration of dissolved ferrous, up to 0.44 mmol L^{-1}, but low concentration of sulphate, below 0.01 mmol L^{-1} (Online Appendix 1). This indicates the anoxic environment in the aquifers and sulphate and iron-oxyhydroxide reduction by organic matters (reactions 11 and 12) should be proceeding.

Table 1 Contribution (%) of the seawater (SW), Red River's water (RW) and local precipitations (LP) to groundwater in Holocene aquifer in study region during rainy and dry seasons

Borehole	Rainy season				Dry season			
	SW	RW	LP	Total	SW	RW	LP	Total
OB-01	36.97	28.49	34.53	100	36.63	43.25	20.12	100
OB-02	53.62	1.34	45.03	100	51.96	22.00	26.03	100
OB-04	61.02	7.98	31.00	100	64.56	14.29	21.15	100
OB-06	12.93	29.91	57.16	100	13.85	37.11	49.04	100
OB-07	0.60	66.59	32.81	100	1.08	88.73	10.19	100
OB-08	2.75	59.12	38.13	100	2.80	65.87	31.33	100
OB-09	0.00	1.67	98.33	100	0.00	5.58	94.43	100
OB-10	4.95	37.17	57.88	100	33.38	29.46	37.16	100
OB-11	19.39	67.71	12.90	100	16.62	76.06	7.32	100
OB-12	5.52	55.15	39.32	100	6.08	56.50	37.43	100
OB-13	48.07	32.23	19.70	100	64.72	19.45	15.83	100
OB-14	32.35	44.51	23.14	100	34.66	49.03	16.32	100
OB-15	10.15	64.36	25.49	100	10.18	78.66	11.16	100
OB-16	0.45	99.62	0.00	100	1.56	98.43	0.00	100

The high salinity and chloride concentration in groundwater of Pleistocene and Neogene aquifers in the NE area could not be explained by salt intrusion neither through the River's bank nor the Ghyben–Herzberg mechanism like in the case of Holocene aquifer aforesaid. It was revealed that the relationships of the $\delta^{18}O$ vs. $[Cl^-]$ as well as the molar $[Na^+]$ to $[Cl^-]$ ratio vs. $[Cl^-]$ for groundwater in Pleistocene and Neogene aquifers within entire study region do not reflect a conservative mixing character of fresh and seawater (Fig. 9a, b).

As seen from Fig. 9a the heavy oxygen isotope composition in groundwater of the deep aquifers varies within a narrow range of $-(7.26‰ \pm 0.76‰)$ whilst the chloride concentration in water does within a wide range, from 22 mmol L^{-1} (Q221a) up to 63 mmol L^{-1} (Q222b). By definition (Eq. 2) the $\delta^{18}O$ signature for seawater should be close to 0‰, therefore if seawater intruded to Pleistocene and Neogene aquifers then the heavy oxygen isotope content in water of those aquifers must be enriched more than $-(7.26‰ \pm 0.76)‰$. On the other hand, results presented in Fig. 7b show the mixing character of young age precipitations with paleo-(old age) water having enriched oxygen-18 signature (Fig. 7b). In fact, it was found that the age of water in Pleistocene and Neogene aquifers in the NE area (Q221a, Q222b, Q224a, Q225a, Q221n, Q223n and Q226n) was from 6 to 14.5 ka old (Online Appendix 2, see Fig. 2 for locations), i.e., the age of the middle and early Holocene. All results presented suggest that brackish and saline waters in Pleistocene and Neogene aquifers in the NE area originated from the entrapped in aquifer and/or aquitard deposits saline pore water which existed since Holocene transgression as it was also pointed out by Bui et al. (2011), Luu et al. (2012) and Nguyen et al. (2014, 2015). Figure 9b is an additional evidence of the diffusive mechanism making water in boreholes Q221a, Q222b, Q224a, Q225a, Q226a, and Q226n in the NE area (see Fig. 2 for locations) to be brackish as the molar $[Na^+]$ to $[Cl^-]$ ratios of water in these boreholes did not vary much (0.73 ± 0.14) within a wide range of $[Cl^-]$ (Fig. 9b). The high concentration of chloride in groundwater of deep aquifers in the NE area associated with the molar $[Na^+]$ to $[Cl^-]$ ratios varying within the range of seawater (0.73 ± 0.14) probably indicates that the migration rate of saline water from the aquifer/aquitard deposits was over the rate of submarine discharge. The rate of two processes apparently depends upon hydraulic conductivity of both aquifer and aquitard deposits.

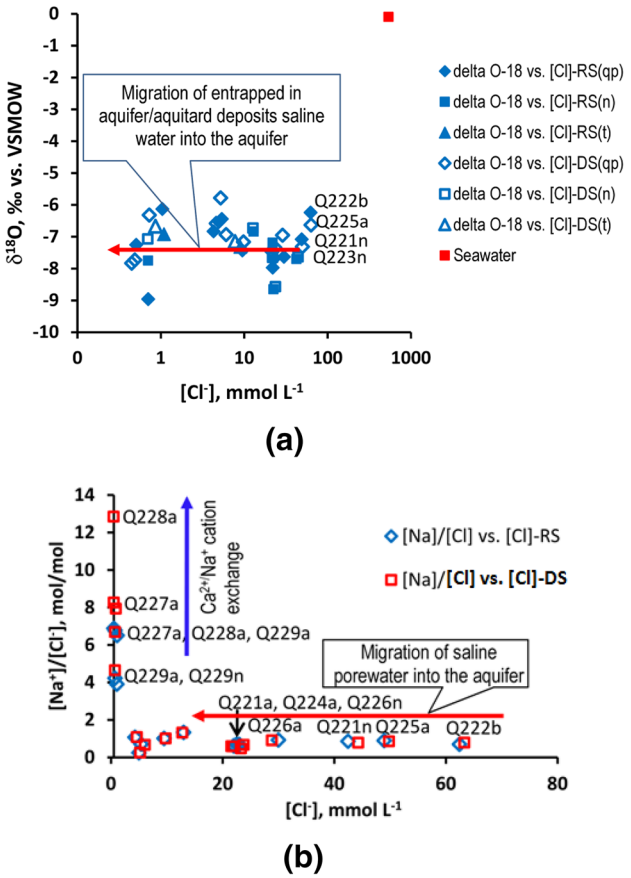

Fig. 9 Relationships of $\delta^{18}O$ vs. molar $[Cl^-]$ (**a**) and molar $[Na^+]$ to $[Cl^-]$ ratios vs. $[Cl^-]$ (**b**) for groundwater in the Pleistocene and Neogene aquifers within the study region showing the migration of entrapped in aquifer and/or aquitard deposits saline porewater to the recharge-fresh water (**a**) as well as the Ca^{2+}/Na^+ cation exchange that proceeds in the areas around the Q227a, Q228a and Q229a boreholes (**b**). **a** was drawn in semi-logarithmic scale (see Fig. 2 for the boreholes locations)

Recently, it has been documented that the hydraulic properties and thickness of the aquitard in the Quaternary Red River Delta plain control recharge and leaching of saline water into Pleistocene aquifer (Larsen et al. 2017). Results from the simulation work of Larsen et al. (2017) allow one to assume that permeability of clayey aquitard in the NE area was higher than that in the SW area. This made the diffusion rate of saline water from the aquitard to Pleistocene aquifer in latter area to be insignificant compared to the rate of the submarine discharge flow hence groundwater in Pleistocene aquifer of the SW area became fresh today. The groundwater of Pleistocene and Neogene aquifers in the SW area have low EC and $[Cl^-]$, except for water from borehole Q109b. Groundwater in Q92, Q108b, Q110a, Q227a, Q228a and Q229a boreholes (see Fig. 2 for the locations) has EC < 1000 µS cm^{-1} and $[Cl^-] < 7$ mmol L^{-1}. The salinity of groundwater around borehole Q109b results from brackish water in the NE flowing to production well field located in proximity of borehole, due to the high mining rate of fresh water from Pleistocene aquifer. This was evident from Fig. 1a that the isolines of water hydraulic head in Pleistocene aquifer were lowdown from −2-m asl in the area close to the Red River to −8-m in area around Q109b borehole.

Chemistry of groundwater in the southern part of the Red River's Delta plain

Sulphate and nitrate ions were found to be in low concentrations in groundwater of Holocene aquifer whilst concentrations of ferrous and ammonia ions were in an elevated range, of up to 0.85 mmol L^{-1} and 5.0 mmol L^{-1}, respectively (in the borehole OB-02 in the RS, Online Appendix 1 and Fig. 4). The [Fe^{2+}] ion found in groundwater tapped from Holocene aquifer in both RS and DS seems to correlate with concentrations of NH_4^+ ion, though $R^2 \sim 0.4$ (figure not shown here), suggesting that reduction of iron-oxyhydroxide by organic matters (reaction 12) is on-going in Holocene aquifer. The relatively weak correlation between [Fe^{2+}] and [NH_4^+] is probably due to the influence of an additional amount of ammonia generated from the biological reduction of nitrate (reaction 13) in the aquifer. In addition, it was found that the [Fe^{2+}] ions in groundwater of the Holocene aquifer were not correlated with [HCO_3^-], i.e., reaction (12) seemingly does not proceed in aquifer. However, calculation of the saturation index (SI) for siderite shows that the $SI_{siderite}$ was (1.52 ± 0.68) and (2.39 ± 0.46) in the rainy and dry season, respectively, implying the mineral is precipitating, thus the concentration of ferrous ion in water would not closely correlate with those of bicarbonate and ammonia.

Results presented in Online Appendix 1 show that the [Ca^{2+}, meq L^{-1}] to [Na^+, meq L^{-1}] ratio for water in Pleistocene and Neogene aquifers in study region ranged from 0.01 to 0.57, which is much lower compared to that ratio for water in the GV01 borehole where groundwater is purely fresh and Ca–HCO_3 type for which the equivalent [Ca^{2+}] to [Na^+] ratio was 28. This finding combined with the results presented in Fig. 9b suggests that cation exchange between calcium ions in groundwater and sodium ions adsorbed on sediment's surface (Appelo and Postma 2007). Figure 9b shows the molar [Na^+] to [Cl^-] ratio in water from boreholes Q227a, Q228a, Q229a and Q229n to be much higher than 0.8, the value representing seawater. This indicates the excess of sodium over chloride concentration is due to the release of sodium from aquifer sediment by Ca^{2+}/Na^+ exchange. To support cation exchange thesis, water chemistry from boreholes Q227a and Q228a is illuminated below.

If there was a conservative mixing of seawater having [Cl^-] and [Na^+] of, respectively, 566 mmol L^{-1} and 485 mmol L^{-1} with fresh groundwater in the RRDP having negligible [Cl^-] and [Na^+] (Postma et al. 2007) then one could calculate concentration of calcium ([Ca^{2+}]) in groundwater of Q227a and Q228a boreholes, based on the material balance as follows:

$$[Ca^{2+}]_{gw} = f_{sea} \times [Ca^{2+}]_{sea} + (1 - f_{sea}) \times [Ca^{2+}]_{fgw}, \quad (18)$$

where [Ca^{2+}] is the concentration of calcium ion in water samples (mmol L^{-1}); f_{sea} is the fraction of seawater; subscripts gw, sea and fgw indicate mixed groundwater sample, seawater and fresh groundwater, respectively.

The fraction of the sea water (f_{sea}) in the mixed groundwater could be calculated based on the concentration of conservative chloride ion similarly to Eq. (18):

$$f_{sea} = \frac{[Cl^-]_{gw} - [Cl^-]_{fgw}}{[Cl^-]_{sea} - [Cl^-]_{fgw}}. \quad (19)$$

In our case the $[Cl^-]_{fgw}$ was negligible compared to the $[Cl^-]_{sea}$, therefore Eq. (19) could be simplified to:

$$f_{sea} = [Cl^-]_{gw}/566. \quad (20)$$

The $[Ca^{2+}]_{sea}$ is 10.7 mmol L^{-1}, while the $[Ca^{2+}]_{fgw}$ in the RRDP was reportedly to be 3.2 mmol L^{-1} (Postma et al. 2007).

By substituting the $[Cl^-]_{gw}$ in groundwater from boreholes Q227a and Q228a (Online Appendix 1) into Eq. (20) one could find fraction of seawater (f_{sea}) mixed with fresh groundwater in the respective boreholes was as large as 10^{-3} and 10^{-2}, if mixings were conservative. Thus, calculated $[Ca^{2+}]_{gw}$ in groundwater from both boreholes Q227a and Q228a deduced from Eq. (18) would be as high as 3.2 mmol L^{-1}. However, the $[Ca^{2+}]_{gw}$ in groundwater from Q227a and Q228a boreholes was measured at 0.2 mmol L^{-1} and 0.01 mmol L^{-1}, respectively (Online Appendix 1). The difference between measured and calculated [Ca^{2+}] in groundwater from boreholes Q227a and Q228a was, respectively, −3.0 to −3.2 mmol L^{-1} meaning Ca^{2+} ion was lost. The similar calculation was made for sodium ion in groundwater from two boreholes with $[Na^+]_{sea} = 485$ mmol L^{-1} and $[Na^+]_{fgw} \cong 0$, and it was that [Na^+] ion in groundwater from boreholes Q227a and Q228a gained, respectively, 3.0 and 4.3 mmol L^{-1}. This is an evidence for Ca^{2+}/Na^+ exchange proceeding in Pleistocene aquifer in study region.

Similarly, a calculation and then comparison with the measured $[SO_4^{2-}]_{gw}$ and $[HCO_3^-]_{gw}$ in groundwater from boreholes Q227a and Q228a assuming the $[SO_4^{2-}]_{sea} = 29.3$ mmol L^{-1}, $[HCO_3^-]_{sea} = 2.3$ mmol L^{-1}; $[SO_4^{2-}]_{fgw} = 5.5$ mmol L^{-1}, $[HCO_3^-]_{fgw} = 10.2$ mmol L^{-1} (Postma et al. 2007) revealed that sulphate in groundwater from the two boreholes was lost, respectively, by −5.3 mmol L^{-1} and −5.5 mmol L^{-1}, whilst the bicarbonate gained by 5.9 and 6.0 mmol L^{-1}. This is the evidence for sulphate reduction (reaction 11) occurring in aquifer. Here one can see that there was no equivalence between gained [Na^+] and lost [Ca^{2+}] or gained [HCO_3^-] and lost [SO_4^{2-}]. For instance, in the groundwater of borehole Q227a, the [Na^+] gained 3.0 mmol L^{-1} vs. [Ca^{2+}] lost −3.0 mmol L^{-1}, and [HCO_3^-] gained 5.9 mmol L^{-1} vs. [SO_4^{2-}] lost −5.3 mmol L^{-1}, while the lost [Ca^{2+}] or [SO_4^{2-}] would be two times lower. However, this could be understood because calcite and dolomite in Pleistocene aquifer are precipitating.

A calculation for the saturation index (SI) of the calcite and dolomite showed that SI_{cc} and SI_{dol} in most water samples in Pleistocene aquifer ranged from 0.01 to 0.5, and from 0.03 to 1.87, respectively, implying saturation and super-saturation of the two minerals (the calculation not shown here). The calcite and dolomite precipitation made the gained $[HCO_3^-]$ and $[Na^+]$ to be imbalanced with lost $[SO_4^{2-}]$ and $[Ca^{2+}]$, respectively.

Figure 10 depicts the relationship between ^{13}C isotopic signature ($\delta^{13}C$) and the molar $[Mg^{2+}]$ to $[Ca^{2+}]$ ratio in groundwater. This graph apparently shows the incongruent dissolution of the high Mg-calcite in Pleistocene aquifer. The incongruent dissolution of biogenic high Mg-calcite (reaction 10) will make the molar $[Mg^{2+}]$ to $[Ca^{2+}]$ ratio to increase (Appelo and Postma 2007; Kloppmann et al. 1998). From the results presented in Online Appendix 1, the molar ratios of $[Mg^{2+}]$ to $[Ca^{2+}]$ in groundwater from study region were computed and it was revealed that these ratios for groundwater tapped from Holocene aquifer ranges from 7.5 to 18.2 in both RS and DS. In water from the Red River $[Mg^{2+}]$ to $[Ca^{2+}]$ ratio is 0.33, and in seawater this ratio is 5.26. This means that $[Mg^{2+}]$ to $[Ca^{2+}]$ ratio in groundwater from Holocene aquifer is 22–55 times higher than that ratio in Red River's water or 1.4–3.4 times higher than that in seawater. In addition, the incongruent dissolution of the high Mg-calcite would lead to enrichment of ^{13}C-signature in DIC (Kloppmann et al. 1998) as seen from Fig. 10 for groundwater in Pleistocene aquifer. However, as can be seen in Fig. 10 increase of molar $[Mg^{2+}]$ to $[Ca^{2+}]$ ratio in groundwater of Pleistocene aquifer was insignificant. This is probably due to the precipitation of calcite and dolomite that could modify the concentration of $[Ca^{2+}]$ and $[Mg^{2+}]$ in groundwater.

The saturation and super-saturation of calcite and dolomite in the Pleistocene aquifer imply that the dissolution of the two minerals (reaction 9) was unimportant in Pleistocene and deeper aquifers. This reaction could be important in the uppermost soil layer where the biogenic carbon dioxide pressure is still high.

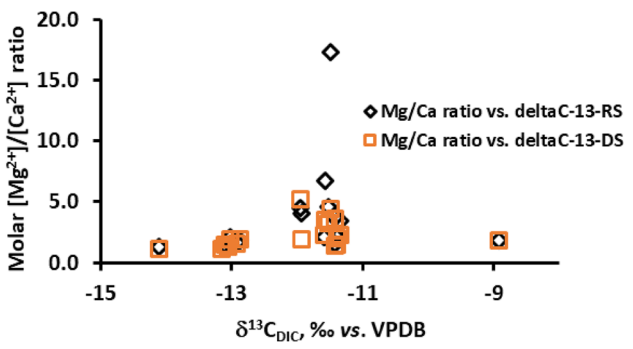

Fig. 10 The relationship of molar $[Mg^{2+}]$ to $[Ca^{2+}]$ ratios vs. $\delta^{13}C$ in DIC showing incongruent dissolution of high Mg-calcite proceeded in the Pleistocene aquifer

Hydraulic interaction between groundwater in different aquifers

A non-parametric, Mann–Whitney test, which allows comparison of independent series of different size without any preliminary hypothesis was applied to examine the hydraulic interaction between the groundwater in different aquifers in study region. In our case, the sample size was large enough to consider that variable built from the test, z, follows a normal distribution. So that difference of means between groups is significant if $z > 1.96$ (critical value at a 5% limit) and very significant if $z > 2.58$ (critical value at a 1% limit). In this case, the mean $\delta^{18}O$ and its standard deviation in the water from Pleistocene, Neogene and Triassic aquifers were used as variables for the test.

It was revealed that mean of $\delta^{18}O$ in water from Pleistocene aquifer was not different from that in water in Neogene and Triassic aquifers, $z = 0.75 < z\text{-critical} = 1.96$ at $\alpha = 0.05$. This implies that water in Pleistocene aquifer connected with those in Neogene and Triassic aquifers and vice versa. This was termed as the inter-aquifer leakage. The inter-aquifer leakage of water between deep aquifers in this case was proven by the water line depicted in Fig. 7b where the isotopic compositions of groundwater from Pleistocene, Neogene and Triassic aquifers positioned along a line characterized for mixing paleo-water of long transit time with water of shorter traveling time. In addition, it was observed that hydraulic head of water in Neogene aquifer monitored in borehole Q109b was always higher than that in Pleistocene aquifer in Q109a borehole for all the time from Jan 1994 to Jan 2018, though the production well field is located in proximity to those boreholes (Fig. 11). This provides another evidence for Pleistocene–Neogene inter-aquifer leakage.

Recharge area, flow direction and flow rate of groundwater in the southern part of the Red River's Delta plain

The recharge to aquifers in the southern part of the Red River's Delta plain is from mountainous areas around GV01 point (Fig. 1a), where the water isotopic composition is close to that of recent precipitations, ^{14}C-content is modern and tritium activity is in the range of 2–3 TU that prevails in the RRDP surface water (Online Appendix 2). There is no recharge to Pleistocene aquifer through the thick Holocene clays, as indicated by high salinity profiles in these clays.

The mean value of $\delta^{18}O$ in groundwater of Pleistocene and Neogene aquifers in study region was −7.25‰ vs. VSMOW (Online Appendix 2), whereas the average $\delta^{18}O$ in precipitations over the RRDP was −8.40‰ vs. VSMOW

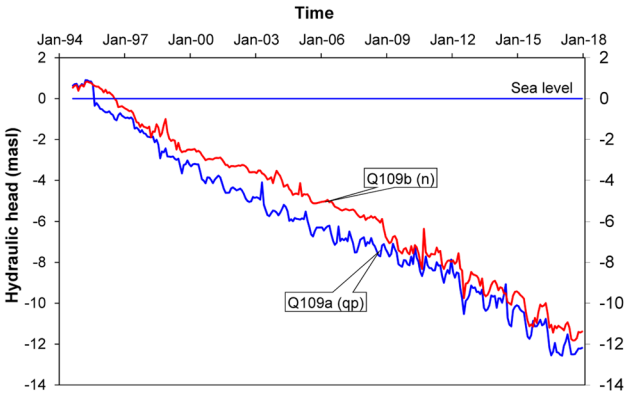

Fig. 11 The hydraulic heads of the groundwater in the Pleistocene and Neogene that have been consecutively monitored in boreholes Q109a and Q109b since 1994 indicating the inter-aquifer leakage between the two aquifers due to the over rate of fresh water mining from the Pleistocene aquifer

(Nhan et al. 2013 and Fig. 8). Thus the difference of mean $\delta^{18}O$ in groundwater of Pleistocene and Neogene aquifers and those in precipitations over the region was − 1.15‰ vs. VSMOW. Considering an altitude gradient of − 0.3‰ per each 100-m rise (Erickson 1983; Mook 2001), the recharge area to Pleistocene and Neogene aquifers in study region was supposed to be a region at about 380-m higher than aquifer altitude or around 150 m above sea level. This area should correspond to the northwest extension of the region and outcrops in Ninh Binh province, i.e., an area around the GV01 point, where the elevation is from 140 to 160-m above sea level (Figs. 1b, 6).

Based on the results of the ^{14}C-dating a conceptual model of groundwater flow in Pleistocene and Neogene aquifers was suggested as depicted in Fig. 6. As seen in Fig. 6, recharge water in study region flows from northwesterly towards southeasterly to the sea, which is in phase with Bui et al. (2011) statement. From Fig. 6 one can see also that groundwater from Neogene and Triassic aquifers is leaking upwards to Pleistocene aquifer making the age of water in the upper aquifer to be older than that of water in the lower aquifers because the leakage needs time to travel from one to another aquifer.

The yield of fresh water mining in recent years in the center of region, in Nam Dinh city, was reportedly to be as high as 95,000 m^3 day^{-1} (Doan 2015) that seems to be over rate of recharge that caused not only inter-aquifer leakage but also could cause backwards flowing of seawater from seaside to well field. Water in borehole Q110 in seaside tapped from Pleistocene aquifer has a ^{14}C-age of 6 ka, almost two times younger than the age (11.3 ka) of water in borehole Q109a installed in proximity of well field (Fig. 6). Apparently, in the SW area seawater is currently intruding into deeper aquifers according to the Ghyben-Herzberg rule making the age of water in boreholes installed at proximity to sea coast to be younger than those inland. Modeling with the use of a MODFLOW model confirmed the scenario (Lindenmaier et al. 2011).

It should be noted that EC of water in borehole Q110 was 825 µS cm^{-1}, which was lower than EC found in the water from boreholes Q109a and Q92a being around 1100 µS cm^{-1} (Online Appendix 1). This implies that saline water in boreholes Q109a and Q92a was not only from the sea but also coming from NE. Results from water head measurements confirmed three flow directions of groundwater in study region. The isolines of water head measured for Pleistocene aquifer are depicted in Fig. 1a. The descent of hydraulic water head delineates direction of water flow. As seen from Fig. 1a, groundwater in study region flows from northwesterly towards southeasterly to the sea, northeasterly towards southwesterly and from the seaside to the production well field in proximity to borehole Q109 as shown by the white arrows (Fig. 1a).

The ineluctable consequence from current over-extraction rate of fresh groundwater in region is that good quality water in the deep aquifers could be under the threat of salt intrusion in future.

Assuming the recharge area is in the highlands around the GV01 point then one can estimate the mean flow rate based on the transit time and distance between recharge area and sampling point. The recharge rate to Neogene aquifer of borehole Q221n was estimated to be as high as 2.5 m a year with a 30 km distance from the recharge area and a water transit time of 11.3 ka.

Conclusion

Groundwater of southern Red River Deltaic plain is found in Holocene, Pleistocene, Neogene and Triassic aquifers. Groundwater in shallow Holocene aquifer is saline and of Na–Cl type and seem to be affected by saltwater intrusion. Groundwater in the Pleistocene, Neogene and Triassic aquifers of SW area is fresh and of Ca–Na–Cl–HCO_3 type, however that occurring across the NE region is brackish and of Na–Ca–Cl type. Higher salinity of groundwater from deep aquifers of NE is due to migration of entrapped saline pore water from aquifer and/or aquitard deposits to aquifers. The hydrogeochemistry of the region is controlled by incongruent dissolution of biogenic Mg-calcite and reduction of sulphate and iron-oxyhydroxide by organic matters of aquifer sediments. The recharge area of deep aquifers is the northwest extension of the study region, at an altitude of 140-160-m above sea level and the flow rate is 2.5 m $year^{-1}$. The extraction rate of fresh water from Pleistocene aquifer was over its recharge rate, thus leading saline water from the seaside to flow backwards to the production well field that

deteriorates the quality of drinking water supplied to local population. Therefore, it is highly advisable that a short-term appropriate strategy for groundwater management in the region is developed and implemented in order to avoid the threat of saltwater intrusion. The most effective measure for preventing seawater intrusion at present is control over groundwater mining at a rate not exceeding current production yield of 95,000 m^3 day^{-1}.

Acknowledgements This research is funded by the Vietnam National Foundation for Science and Technology Development (NAFOSTED) under Grant number 105.99-2014.19. The authors would like to express their sincere thanks to anonymous reviewers for their helpful comments and review of the manuscript.

References

ADB, Asian Development Bank (2016) Viet Nam: water and sanitation sector assessment, strategy and roadmap. Southeast Asia Department working paper, June 2016, Ha Noi

Appelo CA, Postma D (2007) Geochemistry, groundwater and pollution, 2nd edn. A. Balkema Publisher, Amsterdam

Berg M, Tran HC, Nguyen TC, Pham HV, Schetenleib R, Riger W (2001) Arsenic contamination of groundwater and drinking water in Vietnam: a human health threat. Environ Sci Technol 25:2621–2626

Bigeleisen CT, Mayer MG (1947) Calculation of equilibrium constants for isotopic exchange reactions. J Chem Phys 15:261–270

Bui DD, Kawamura A, Tong NT, Amaguchi H, Nakagawa N, Iseri Y (2011) Identification of aquifer system in the whole Red River Delta, Vietnam. Geosci J 15:323–338

Clark ID, Fritz P (1997) Environmental isotopes in hydrology. Lewis Publisher, New York

Clark ID, Fritz P, Michel FA, Southern JG (1982) Isotope hydrogeology and geothermometry of the Mount Meager geothermal area. Can J Earth Sci 19:1454–1473

Craig H (1961) Isotopic variation in meteoric water. Science 133:1702–1703

Doan VC (2015) Investigation to propose criteria and zones for sustainable exploitation and protection of the groundwater resources in the Red River's (Bac Bo) and the Mekong River's (Nam Bo) deltas. Final report to the Ministry of Science and Technology (Vietnam) for the Research Program, Ha Noi **(in Vietnamese)**

Erickson E (1983) Stable isotopes and tritium in precipitation. Guidebook on Nuclear Techniques in Hydrology. IAEA Technical Report Series No. 91, Vienna, Austria, pp 19–33

Fontes JC (1983) Dating of groundwater. Guidebook on Nuclear Techniques in Hydrology. IAEA Technical Report Series No. 91, Vienna, Austria, pp 285–317

Fontes, JC, Garnier JM (1979) Determination of the initial activity of the total dissolved carbon: a review of the existing models and a new approach. Water Resour Res 12:399–413

Frenken K (ed) (2012) Irrigation in Southern and Eastern Asia in figures. Food and Agriculture Organization of the United Nations (FAO) Report No. 37, Rome

Glynn PD, Plummer LN (2005) Geochemistry and the understanding of groundwater systems. Hydrogeol J 13:263–287

Groening M, Dargier M, Tatzber H (2004) Seventh IAEA intercomparison of low-level tritium measurement in water (TRIC-2004). International Atomic Energy Agency, Vienna, 2007. http://www-naweb.iaea.org/napc/ih/documents/IHL/TRIC/TRIC2004-Report.pdf. Accessed Dec 2016

Groening M, Tatzber H, Trinkl A, Klaus B, van Duren M (2008) Eighth IAEA intercomparison of low-level tritium measurement in water (TRIC-2008). International Atomic Energy Agency, Vienna, 2009. http://www-naweb.iaea.org/napc/ih/documents/IHL/TRIC/TRIC2008-Report.pdf. Accessed Dec 2016

Gupta SK, Polach HA (1985) Radiocarbon dating practices at ANU. Radiocarbon Laboratory, Research School of Pacific Studies, ANU, Canberra

Hoang VH (2014) Salt water intrusion in Quaternary sediment in Nam Dinh area. Ph.D. Thesis, Hanoi University of Mining and Geology, Vietnam **(in Vietnamese)**

IAEA, International Atomic Energy Agency (2002) Water and environment newsletter of the Isotope Hydrology Section, International Atomic Energy Agency. Issue No. 16, Nov. 2002

Kalin RM (2000) Radiocarbon dating of groundwater systems. In: Cook PG, Herczeg AL (eds) Environmental tracers in subsurface hydrology. Springer, Boston

Kasbohm J, Grothe S, Le Thi LAI (2013) Province Nam Dinh an analysis for a future integrated water resource management. http://www.idm.gov.vn. Accessed 21 Aug 2017

Kloppmann W, Dever L, Edmunds WM (1998) Residence time of Chalk groundwaters in the Paris Basin and the North German basin: a geochemical approach. Appl Geochem 13:593–606

Koln JM (2010) Carbon isotope compositions of terrestrial C3 plants as indicators of (paleo)ecology and (paleo)climate. Proc Natl Acad Sci USA 107:19691–19695. https://doi.org/10.1073/pnas.1004933107

Larsen F, Pham NQ, Dang ND, Postma D, Jessen S, Pham VH, Nguyen TB, Trieu HD, Tran LT, Nguyen H, Chambon J, Nguyen HV, Ha DH, Hue NT, Duc MT, Refsgaard JC (2008) Controlling geological and hydrogeological processes in an arsenic contaminated aquifer on the Red River flood plain. Vietnam. Appl Geochem 23(11):3099–3115

Larsen F, Long VT, Hoan HV, Luu TT, Christiansen AV, Nhan PQ (2017) Groundwater salinity influenced by Holocene seawater trapped in incised valleys in the Red River Delta plain. Nat Geosci. https://doi.org/10.1038/NGEO2938

Le TL, Doan VC (2005) Nitrogen compounds and iron contamination in the groundwater of the Holocene aquifer in the Nam Dinh area. J Geol Ser B 25:43–51

Le VH, Bui H, Chau VQ, Dang HO, Le HH, Nguyen TT, Tran M (2000) Groundwater in the Bac Bo Plain (North Vietnam). A technical report to the General Department of Geology and Minerals of Viet Nam, Ha Noi **(in Vietnamese)**

Lindenmaier F, Bahls R, Wagner F (2011) Assessment of groundwater resources in Nam Dinh Province. Final Technical Report, Part B: three dimensional structural and numerical modelling, Hanoi

Luu TMN, Garnier J, Billen G, Orange D, Nemery J, Le TPQ, Tran HT, Le LA (2010) Hydrological regime and water budget of the Red River Delta (Northern Vietnam). J Asian Earth Sci 37:219–228

Luu T, Tran F, Larsen NQ, Pham AV, Christiansen N, Tran HV, Vu LV, Tran HV, Hoang, Hinsby K (2012) Origin and extent of fresh groundwater, salty paleowaters and recent saltwater intrusions in the Red River flood plain aquifers. Vietnam Hydrogeol J 20:1295–1313

Mann WB (1983) An international reference material for radiocarbon dating. Radiocarbon 25:519–522

McArthur JM, Banerjee DM, Hudson-Edwards KA, Mishra R, Purohit R, Ravenscroft P, Cronin A, Howarth RJ, Chatterjee A, Talukder T, Lowry D, Houghton S, Chadha DK (2004) Natural organic matter in sedimentary basins and its relation to arsenic in anoxic groundwater: the examples of West Bengal and its worldwide implications. Appl Geochem 19:1255–1293

Mook WG (ed) (2001) Environmental isotopes in the hydrological cycle. Principles and applications. Atmospheric water, vol II. IAEA, Vienna

Mook WG, Bommerson JC, Staverman WH (1974) Carbon isotope fractionation between dissolved and gaseous carbon dioxide. Earth Planet Sci Lett 22:169–176

NCMH, National Center for Monitoring the Hydrology in the Marine Coast (2012) The hydrological regime along the marine coast, North Vietnam in the 2012 year. Annual report to the General Directorate of Meteorology and Hydrology of Vietnam, Ha Noi

NDPSO, Nam Dinh Province Statistical Office (2014) Area and Population of the province. http://www.gso.gov.vn. Accessed 10 Apr 2017

Nguyen VH (2009) Investigation into the rainwater recharge to the Holocene aquifer in the Ha Noi area by using isotopic and related techniques. MSc Thesis, Hanoi University of Mining and Geology, Ha Noi **(in Vietnamese)**

Nguyen DN, Nguyen TH (2004) Climate and climate resources in Vietnam. Agriculture Publishing House, Ha Noi **(in Vietnamese)**

Nguyen TT, Kawamura A, Tong NT, Nakagawa N, Amaguchi H, Gilbuena R Jr (2014) Hydrogeochemical characteristics of groundwater from the two aquifers in the Red River Delta, Vietnam. J Asian Earth Sci. https://doi.org/10.1016/j.jseaes.2014.07.035

Nguyen TT, Kawamura A, Tong NT, Nakagawa N, Amaguchi H, Gilbuena R Jr (2015) Clustering spatio-seasonal hydrogeochemical data using self-organizing maps for groundwater quality assessment in the Red River Delta, Vietnam. J Hydrol 522:661–673

Nhan DD, Lieu DB, Minh DA, Anh VT (2013) Isotopic composition of the precipitations over the Ha Noi city (Vietnam) region: data of the GNIP Ha Noi. http://www.iaea/gnip. Accessed Dec 2016

Noakes JE, Kim S, Akers L (1967) Recent improvements in benzene chemistry for radiocarbon dating. Geochim Cosmochim Acta 31:1094–1096

Norrman J, Sparrenbom CJ, Berg M, Nhan DD, Nhan PQ, Rosqvist H, Jacks G, Sigvardsson E, Baric D, Moreskog J, Harms-Ringdahl P, Hoan NV (2008) Arsenic mobilisation in a new well field for drinking water production along the Red River, Nam Du, Hanoi. Appl Geochem 23:3127–3142

Norrman J, Sparrenbom CJ, Berg M, Dang DN, Jacks G, Harms-Ringdahl P, Pham QN, Rosqvist H (2015) Tracing sources of ammonium in reducing groundwater in a well field in Hanoi (Vietnam) by means of stable nitrogen isotope ($\delta^{15}N$) values. Appl Geochem 61:248–258

Pham QS (2004) Study for development of the Red River–That Binh River's estuaries using remote sensing information and GIS techniques to support rational exploitation of natural resources in the region. Ph.D. Dissertation. Ha Noi National University, Ha Noi **(in Vietnamese)**

Plastino W, Chereji I, Cuna S, Kaihola L, de Felice P, Lupsa N, Balas G, Mirel V, Berdea P, Baciu C (2007) Tritium in water electrolytic enrichment and liquid scintillation counting. Radiat Meas 42:68–73

Plummer NL, Prestemon EC, Parkhurst DL (1994) An interactive code (NETPATH) for modeling net geochemical reactions along a flow path, version 2.0. US Geological Survey Water Resources Investigations Report 94-4169. USGS, Reston

Postma D, Larsen F, Nguyen TMH, Mai TD, Pham HV, Pham QN, Jessen S (2007) Arsenic in groundwater of the Red River floodplain, Vietnam: controlling geochemical processes and reactive transport modelling. Geochim Cosmochim Acta 71:5054–5071

Salem O, Visser JM, Deay M, Gonfiantini R (1980) Groundwater flow patterns in the western Libyan Arab Jamahitiya evaluated from isotope data. In: Arid zone hydrology: investigation with isotope techniques. Proc. of an advisory group meeting on application of isotope techniques in arid zones hydrology. IAEA, Vienna, Austria, 6–9 Nov, 1978. Paper No. IAEA-AG-158/12, pp 165–179

Sánchez-Murillo R, Brooks ES, Elliot WJ, Boll J (2015) Isotope hydrology and baseflow geochemistry in natural and human-altered watersheds in the Inland Pacific Northwest, USA. Isot Environ Health Stud 51: 231–254

Stiefel JM, Melesse AM, McClain ME, Price RM, Anderson EP, Chauhan NK (2009) Effects of rainwater-harvesting-induced artificial recharge on the groundwater of wells in Rajasthan, India. Hydrogeol J 17(8):2061–2073

Stookey LL (1970) Ferrozine—a new spectrophotometric reagent for iron. Anal Chem 42:779–781

Stumm W, Morgan JJ (1981) Aquatic chemistry, 2nd edn. Wiley & Sons, New York

Tamers MA (1975) Chemical yield optimization of the benzene synthesis for radiocarbon dating. Int J Appl Radiat Isot 26(11):676–682

Tanabe S, Hori K, Saito Y, Haruyama S, Doanh LQ, Sato Y, Hiraide S (2003) Sedimentary facies and radiocarbon dates of the Nam Dinh-1 core from the Song Hong (Red River) delta, Vietnam. J Asian Sci 21:503–513

Villa M, Manjon G (2004) Low-level measurements of tritium in water. Appl Radiat Isot 61(2–3):319–323

Wagner F, Trung DT, Phuc HD, Lindenmaier F (2011) Assessment of groundwater resources in Nam Dinh province. Final technical report for the IGPVN Project. Part A, Hanoi, Vietnam

Zheng Y, Stute M, van Geen A, Gavrieli I, Dhar R, Simpson HJ, Schlosser P, Ahmed KM (2004) Redox control of arsenic mobilization in Bangladesh groundwater. Appl Geochem 19:201–214

Zhu C (2000) Estimate of recharge from radiocarbon dating of groundwater and numerical flow and transport modeling. Water Resour Res 36:2607–2620